Multifield mimetic gravity

Seyed Ali Hosseini Mansoori,[1,*] Alireza Talebian,[2,†] Zahra Molaee,[2,‡] and Hassan Firouzjahi[2,§]

[1]*Faculty of Physics, Shahrood University of Technology, P.O. Box 3619995161 Shahrood, Iran*
[2]*School of Astronomy, Institute for Research in Fundamental Sciences (IPM), P.O. Box 19395-5531, Tehran, Iran*

(Received 8 October 2021; accepted 14 January 2022; published 26 January 2022)

In this paper, we extend the mimetic gravity to the multifield setup with a curved field space manifold. The multifield mimetic scenario is realized via the singular limit of the conformal transformation between the auxiliary and the physical metrics. We look for the cosmological implications of the setup where it is shown that at the background level the mimetic energy density mimics the roles of dark matter. At the perturbation level, the scalar field perturbations are decomposed into the tangential and normal components with respect to the background field space trajectory. The adiabatic perturbation tangential to the background trajectory is frozen while the entropy mode perpendicular to the background trajectory propagates with the speed of unity. Whether or not the entropy perturbation is healthy directly depends on the signature of the field-space metric. We perform the full nonlinear Hamiltonian analysis of the system with the curved field space manifold and calculate the physical degrees of freedom verifying that the system is free from the Ostrogradsky-type ghost.

DOI: 10.1103/PhysRevD.105.023529

I. INTRODUCTION

Over the years, there have been interests in theories of modified gravity as possible solutions to some unsolved problems in cosmology and general relativity (GR) like the dark matter, dark energy, the singularity problem, and so on. Recently, the mimetic gravity has been proposed as a modification of GR that may mimic the roles of dark matter [1–4]. Mimetic gravity may be realized by performing a noninvertible conformal transformation of the physical metric $g_{\mu\nu}$ in the Einstein-Hilbert action from an auxiliary metric $\tilde{g}_{\mu\nu}$ via $g_{\mu\nu} = -(\tilde{g}^{\alpha\beta}\partial_\alpha\phi\partial_\beta\phi)\tilde{g}_{\mu\nu}$ in which ϕ is a scalar field [5–7]. In this way, the scalar field satisfies the constraint[1]

$$g^{\mu\nu}\partial_\mu\phi\partial_\nu\phi = -1. \tag{1.1}$$

With this constraint, the theory reproduces the behavior of a pressureless fluid on a cosmological scale and therefore yields a candidate of the dark matter. Alternatively, the mimetic gravity can be equivalently constructed by adding the above mimetic constraint via a Lagrange multiplier into the action. For various studies on mimetic gravity setups, see Refs. [8–42].

In spite of the fact that the original mimetic theory is free from instabilities [43,44], there is no nontrivial dynamics for scalar perturbations. This may result in caustic problem in the mimetic dark matter scenario [45–49]. To remedy this issue, the higher derivative term $(\Box\phi)^2$ may be added to the action causing the scalar perturbations to propagate with a nonzero sound speed [2,8]. Correspondingly, the mimetic setup with a general higher derivative function in the form $f(\Box\phi)$ has also been studied in Refs. [3,4]. However, this extension of the mimetic setup with a higher derivative $f(\Box\phi)$ suffers from the ghost and the gradient instabilities [50,51]. To find a way of resolving the above problems, it was demonstrated in [52–54] that it is possible to bypass both gradient and the ghost instabilities by introducing direct couplings of the higher derivative terms to the curvature tensor of the spacetime. In this respect, more recently, the inflationary solutions in the healthy setup of extended mimetic gravity with the inclusion of higher derivative terms and the curvature tensor of spacetime were constructed in [55].

The two-field extension of the mimetic gravity in the singular conformal limit of the disformal transformation has been studied in [7]. By decomposing the perturbations into the adiabatic and entropy modes, it was also shown that, similar to the original single field mimetic model, the adiabatic mode is frozen, whereas the entropy mode propagates with the sound speed equal unity with no ghost and gradient instabilities. In addition, the shift symmetry condition imposed in two mimetic fields setup leads to the Noether current, which provides a dark-matter-like energy

*shosseini@shahroodut.ac.ir
†talebian@ipm.ir
‡zmolaee@ipm.ir
§firouz@ipm.ir

[1]Here, we use the mostly positive signature for the spacetime metric.

density component at the cosmological background. By imposing the shift symmetries on both scalar fields ϕ^1 and ϕ^2, the corresponding two-field mimetic constraint is given by

$$c_1 g^{\mu\nu}\partial_\mu\phi^1\partial_\nu\phi^1 + c_2 g^{\mu\nu}\partial_\mu\phi^2\partial_\nu\phi^2 = -1, \qquad (1.2)$$

in which c_1 and c_2 are positive constants [7]. Without a loss of generality, these constants can be absorbed into the fields through the field redefinitions $\phi^1 \to \phi^1/\sqrt{c_1}$ and $\phi^2 \to \phi^2/\sqrt{c_2}$, so the above mimetic constraint can be written in the covariant form

$$\delta_{ab} g^{\mu\nu}\partial_\mu\phi^a\partial^\mu\phi^b = -1, \quad \text{with} \quad \phi^a = (\phi^1, \phi^2). \qquad (1.3)$$

Written in this form, one can think of δ_{ab} as a metric characterizing a flat geometry of the target space spanned by the fields $\phi^a = (\phi^1, \phi^2)$. This was a consequence of the shift symmetry imposed in field space.

In this work we build upon [7] and consider a setup of multifield mimetic gravity with a curved field space metric $G_{ab}(\phi^c)$. As such, the shift symmetry assumption is violated. The dynamics of such multifield models with a curved field-space manifold have been extensively studied in recent years mainly in the context of inflation, dark energy, primordial non-Gaussianity, and related areas [56–65].

The rest of the paper is organized as follows. In Sec. II we present the multifield extension of the original mimetic scenario. In Sec. III we study the cosmological implications of the setup both at the background and the perturbations levels. In Sec. IV, we perform the Hamiltonian analysis at the full nonlinear level using the Arnowitt-Deser-Misner (ADM) decomposition [66]. The conclusions are presented in Sec. V while some technicalities of the analysis are relegated to the Appendixes.

II. THE MODEL

In this section, we build upon the analysis of [7] and construct the mimetic setup for the general case of multifield with a curved field space metric G_{ab}. We comment that the setup of [7] was dealing with a two-field setup with a flat field space, i.e., $G_{ab} = \delta_{ab}$, with the constraint given by Eq. (1.2).

To do this, let us first assume a general conformal transformation between the physical metric $g_{\mu\nu}$ and the auxiliary metric $\tilde{g}_{\mu\nu}$ as

$$g_{\mu\nu} = A(\phi^a, X)\tilde{g}_{\mu\nu}, \qquad (2.1)$$

where $X = G_{ab}\tilde{g}^{\mu\nu}\partial_\mu\phi^a\partial_\nu\phi^b$ in which $G_{ab}(\phi^c)$ is the metric of the field-space manifold.[2] Demanding that the determinant of $g_{\mu\nu}$ to be nonzero, its inverse metric is given by $g^{\mu\nu} = A^{-1}\tilde{g}^{\mu\nu}$. In order to find if the above transformation is invertible, we need to look at the eigenvalue equation for the determinant of the Jacobian [67], i.e.,

$$\left(\frac{\partial g_{\mu\nu}}{\partial \tilde{g}_{\mu\nu}} - \kappa^{(n)}\delta^\alpha_\mu\delta^\beta_\nu\right)\xi^{(n)}_{\alpha\beta} = 0, \qquad (2.3)$$

in which $\kappa^{(n)}$ and $\xi^{(n)}_{\mu\nu}$ are the eigenvalues and the associated eigentensors, respectively. Therefore, the eigenvalues equation for the conformal transformation (2.1) can be obtained to be

$$(A - \kappa^{(n)})\xi^{(n)}_{\mu\nu} - A_{,X}\langle\xi^{(n)}\rangle_X \tilde{g}_{\mu\nu} = 0, \qquad (2.4)$$

where we have defined $\langle\xi^{(n)}\rangle_X \equiv G_{ab}\partial^\alpha\phi^a\partial^\beta\phi^b\xi^{(n)}_{\alpha\beta}$. The above relation can be proved by using the following identities:

$$\frac{\partial g_{\mu\nu}}{\partial \tilde{g}_{\alpha\beta}} = A\delta^\alpha_\mu\delta^\beta_\nu + \tilde{g}_{\mu\nu}\frac{\partial A}{\partial \tilde{g}_{\alpha\beta}}, \qquad (2.5)$$

where

$$\frac{\partial A}{\partial \tilde{g}_{\alpha\beta}} = G_{ab}\delta^\alpha_\rho\delta^\beta_\sigma\partial^\rho\phi^a\partial^\sigma\phi^b A_{,X}. \qquad (2.6)$$

There are usually two kind of solutions for this eigenvalues that are known as the "conformal type solution" and the "kinetic type solution." In the case of conformal type solution, the eigenvalues and eigentensor are given by

$$\kappa^{(C)} = A \quad \text{with} \quad A_{,X}\langle\xi^{(C)}\rangle_X = 0. \qquad (2.7)$$

Clearly, this kind of eigenvalue solution is degenerate with a multiplicity of 9 since the eigentensors are limited by the above (single) constraint. On the other hand, for the kinetic type eigenvalues solution, we have

$$\kappa^{(K)} = A - XA_{,X}, \qquad (2.8)$$

with the eigentensor being proportional to the metric tensor, i.e., $\xi^{(K)}_{\mu\nu} = \tilde{g}_{\mu\nu}$.

Now we are interested in finding the singular limit of the conformal transformation (2.1) by demanding that the

[2]The natural generalization of disformal transformation in the case of multifield mimetic gravity can be expressed by

$$g_{\mu\nu} = A(\phi^a, X)\tilde{g}_{\mu\nu} + C(\phi^a, X)G_{ab}\partial_\mu\phi^a\partial_\nu\phi^b. \qquad (2.2)$$

Note that we take $C = 0$ in the conformal case.

eigenvalues (2.8) and/or (2.7) to be zero. In the case of conformal type solution, the singular limit gives us $A = 0$, which is not allowed. However, for the kinetic type solution, the following constraint will be imposed on A in the singular limit,

$$A = XA_{,X}. \tag{2.9}$$

The nontrivial solution of the above differential equation for the conformal factor A is

$$A = -\Omega^{-1}X, \tag{2.10}$$

in which Ω is a constant. Therefore, A is obtained to be a linear function of X. There are two options for the sign of Ω. If we assume that the mimetic fields are timelike, which is the case for the cosmological background, then $X < 0$, so we need $\Omega > 0$. On the other hand, if the mimetic fields are spacelike, as for example in the black hole background studied in [68], then $\Omega < 0$. We are interested in cosmological implications of the multifield mimetic gravity, so we assume $\Omega > 0$.

It is worth mentioning that one cannot write down $\tilde{g}_{\mu\nu}$ as a function of $g_{\mu\nu}$ due to the nature of the above singular limit. By contracting both sides of the inverse metric relation, $g^{\mu\nu} = -\Omega X^{-1}\tilde{g}^{\mu\nu}$ with $G_{ab}\partial^\mu\phi^a\partial_\nu\phi^b$, one obtains

$$g^{\mu\nu}G_{ab}\partial_\mu\phi^a\partial_\nu\phi^b = -\frac{\Omega G_{ab}\partial_\mu\phi^a\partial_\nu\phi^b\tilde{g}^{\mu\nu}}{X}, \tag{2.11}$$

which yields

$$g^{\mu\nu}G_{ab}\partial_\mu\phi^a\partial_\nu\phi^b = G_{ab}\partial_\mu\phi^a\partial^\mu\phi^b = -\Omega. \tag{2.12}$$

This is nothing but the mimetic constraint extended to curved multifield manifold.

The above constraint can be applied to the theory via a Lagrange multiplier. For the single field mimetic gravity setup, it has been shown that the conformal transformation of the metric to an auxiliary metric is equivalent to adding a Lagrange multiplier to the action [69]. But for the multifield case in curved space, this conclusion might be unclear. In the next subsection, we demonstrate that these two approaches are equivalent in the multifield case as well.

A. Equivalent action with a Lagrange multiplier

Here, our aim is to show that the action constructed from the physical metric (2.1) is equivalent with the action in which the mimetic constraint (2.12) is added to it through a Lagrange multiplier in the following form

$$S = \int d^4x\sqrt{g}\left[\frac{M_P^2}{2}R + \lambda(G_{ab}\partial_\mu\phi^a\partial^\mu\phi^b + \Omega) - V(\phi^a)\right], \tag{2.13}$$

in which M_P is the reduced Planck mass, λ is the Lagrange multiplier, and $V(\phi^a)$ is the potential added for the later cosmological purposes. As mentioned, the equivalency of the two actions for the case of single field mimetic scenario was shown in [69] and we follow its logic here (with some new technicalities coming from multifield effects).

From Eqs. (2.1) and (2.10), we consider the physical metric $g_{\mu\nu}$ as a function of auxiliary $g_{\mu\nu}$ and scalar fields ϕ^a as

$$g_{\mu\nu} = -\Omega^{-1}(G_{ab}\tilde{g}^{\alpha\beta}\partial_\alpha\phi^a\partial_\beta\phi^b)\tilde{g}_{\mu\nu} \equiv -\Omega^{-1}X\tilde{g}_{\mu\nu}. \tag{2.14}$$

Clearly, the metric $g_{\mu\nu}$ is invariant under the conformal transformation of the auxiliary metric $\tilde{g}_{\mu\nu}$.

The action constructed from the physical metric $g_{\mu\nu}$ can be considered as a function of scalar fields ϕ^a and the auxiliary metric $\tilde{g}_{\mu\nu}$ as follows

$$S = \int d^4x\sqrt{-g(\tilde{g}_{\mu\nu},\phi^a)}\left(\frac{M_P^2}{2}R(g_{\mu\nu}(\tilde{g}_{\mu\nu},\phi^a)) + \mathcal{L}_m\right), \tag{2.15}$$

where $\mathcal{L}_m$ represents the Lagrangian density of the matter sector, which for our case is just the potential $V(\phi^a)$.

By taking the variation of the action with respect to the physical metric $g_{\mu\nu}$, we arrive at

$$\delta S = \frac{1}{2}\int d^4x\sqrt{-g}(M_P^2\mathcal{G}^{\mu\nu} - T^{\mu\nu})\delta g_{\mu\nu}, \tag{2.16}$$

in which $\mathcal{G}^{\mu\nu}$ is the Einstein tensor and $T^{\mu\nu}$ is the energy-momentum tensor associated to $\mathcal{L}_m$.

From Eq. (2.14) the variation $\delta g_{\mu\nu}$ can be written in terms of the variation of the auxiliary metric $\delta\tilde{g}_{\mu\nu}$ and the variation of scalar field $\delta\phi^a$ as follows

$$\delta g_{\mu\nu} = -\frac{X}{\Omega}\delta\tilde{g}_{\mu\nu} - \frac{\delta X}{\Omega}\tilde{g}_{\mu\nu}, \tag{2.17}$$

$$\begin{aligned} &= -\frac{X}{\Omega}\delta\tilde{g}_{\mu\nu} - \frac{\tilde{g}_{\mu\nu}}{\Omega}(XG_{ab,c}\delta\phi^c \\ &\quad + G_{ab}[-\tilde{g}^{\kappa\alpha}\tilde{g}^{\rho\beta}\delta\tilde{g}_{\alpha\beta}\partial_\kappa\phi^a\partial_\rho\phi^b + 2\tilde{g}^{\kappa\rho}\partial_\kappa\delta\phi^a\partial_\rho\phi^b]), \\ &= -\frac{X}{\Omega}\delta\tilde{g}_{\alpha\beta}\left(\delta^\alpha_\mu\delta^\beta_\nu + \frac{G_{ab}}{\Omega}g_{\mu\nu}g^{\kappa\alpha}g^{\rho\beta}\partial_\kappa\phi^a\partial_\rho\phi^b\right) \\ &\quad - \frac{g_{\mu\nu}}{\Omega}(G_{ab,c}X^{ab}\delta\phi^c + 2G_{ab}g^{\kappa\rho}\partial_\kappa\delta\phi^a\partial_\rho\phi^b), \end{aligned} \tag{2.18}$$

where $X^{ab} \equiv g^{\alpha\beta}\partial_\alpha\phi^a\partial_\beta\phi^b$.

Thus the corresponding equations of motion from the variation in Eq. (2.16) are obtained to be

$$\begin{aligned} &\mathcal{G}_{\mu\nu} - T_{\mu\nu} + \Omega^{-1}(\mathcal{G} - T)G_{ab}\partial_\mu\phi^a\partial_\nu\phi^b = 0, \\ &(\mathcal{G} - T)G_{ab,c}X^{ab} - 2\nabla_\kappa((\mathcal{G} - T)G_{ac}\nabla^\kappa\phi^a) = 0. \end{aligned} \tag{2.19}$$

By taking the trace of Eq. (2.18), we have

$$(\mathcal{G} - T)(G_{ab}\partial_\mu\phi^a\partial^\mu\phi^b + \Omega) = 0. \tag{2.20}$$

When $\mathcal{G} - T \neq 0$, this equation yields the mimetic constraint (2.12).

On the other hand, instead of working with the action (2.15) with the physical metric $g_{\mu\nu}$ treated as a function of the auxiliary metric $\tilde{g}_{\mu\nu}$ and the scalar fields ϕ^a, we can equivalently implement the relation (2.14) to the total action with a set of Lagrange multipliers and treat $g_{\mu\nu}$ as an independent field, i.e.,

$$S = \int d^4x\sqrt{-g}\left[\frac{M_P^2}{2}R + \Lambda^{\mu\nu}(g_{\mu\nu} + \Omega^{-1}X\tilde{g}_{\mu\nu}) + \mathcal{L}_m\right]. \tag{2.21}$$

Here $\Lambda^{\mu\nu}$ is a set of Lagrangian multipliers added to incorporate the condition (2.15) for all components of metric field. Consequently, the variation of action with respect to $\Lambda_{\mu\nu}$ yields the constraint (2.14). Note that despite the apparent similarity, the constrained action (2.21) is different than the constrained action (2.13). More specifically, the single Lagrange multiplier λ in action (2.13) enforces the single constraint Eq. (2.12) while the Lagrange multipliers $\Lambda^{\mu\nu}$ implement the relation (2.14) for all components of the physical metric.

Now the variation of action (2.21) is given by

$$\begin{aligned} \delta S &= \frac{1}{2}\int d^4x\sqrt{-g}[(\mathcal{G}^{\mu\nu} - T^{\mu\nu} + \Lambda^{\mu\nu})\delta g_{\mu\nu} + \Omega^{-1}\Lambda^{\mu\nu}\delta\tilde{g}_{\mu\nu}X + \Omega^{-1}\Lambda^{\mu\nu}\tilde{g}_{\mu\nu}\delta X], \\ &= \frac{1}{2}\int d^4x\sqrt{-g}[(\mathcal{G}^{\mu\nu} - T^{\mu\nu} + \Lambda^{\mu\nu})\delta g_{\mu\nu} + \Omega^{-1}(\Lambda G_{ab,c}X^{ab} - 2\nabla_\kappa(\Lambda G_{ac}\nabla^\kappa\phi^a))\delta\phi^c] \\ &\quad + \Omega^{-1}\Lambda^{\mu\nu}X(\delta^\alpha_\mu\delta^\beta_\nu + \Omega^{-1}G_{ab}g_{\mu\nu}g^{\kappa\alpha}g^{\rho\beta}\partial_\kappa\phi^a\partial_\rho\phi^b)\delta\tilde{g}_{\alpha\beta}, \end{aligned} \tag{2.22}$$

where $\Lambda \equiv \Lambda^{\mu\nu}g_{\mu\nu}$ and we have set the boundary contribution to zero by demanding that the variation of $\delta\phi^b$ vanishes at infinity. In addition, use was made from the following relation,

$$\begin{aligned} \delta X &= G_{ab,c}\tilde{g}^{\alpha\beta}\partial_\alpha\phi^a\partial_\beta\phi^b\delta\phi^c + G_{ab}(-\tilde{g}^{\kappa\alpha}\tilde{g}^{\rho\beta}\delta\tilde{g}_{\alpha\beta}\partial_\kappa\phi^a\partial_\rho\phi^b + 2\tilde{g}^{\kappa\rho}\partial_\kappa\delta\phi^a\partial_\rho\phi^b), \\ &= -\Omega^{-2}X^2G_{ab}g^{\kappa\alpha}g^{\rho\beta}\partial_\kappa\phi^a\partial_\rho\phi^b\delta\tilde{g}_{\alpha\beta} - \Omega^{-1}X(G_{ab,c}X^{ab}\delta\phi^c + 2G_{ab}g^{\kappa\rho}\partial_\kappa\delta\phi^a\partial_\rho\phi^b). \end{aligned} \tag{2.23}$$

Now the variations in Eq. (2.22) with respect to the physical metric $g_{\mu\nu}$, the auxiliary metric $\tilde{g}_{\mu\nu}$ and the scalar fields ϕ^a, respectively, lead to

$$\mathcal{G}_{\mu\nu} - T_{\mu\nu} + \Lambda_{\mu\nu} = 0, \tag{2.24}$$

$$\Lambda_{\mu\nu} + \Omega^{-1}\Lambda G_{ab}\partial_\mu\phi^a\partial_\nu\phi^b = 0, \tag{2.25}$$

$$\Lambda G_{ab,c}X^{ab} - 2\nabla_\kappa(\Lambda G_{ac}\nabla^\kappa\phi^a) = 0. \tag{2.26}$$

Interestingly, the trace of Eq. (2.25) leads to the mimetic constraint (2.12). Moreover, by taking the trace from Eq. (2.24), we find that $\Lambda = T - \mathcal{G}$. Therefore, using this finding and substituting Eq. (2.25) into (2.24), the equation of motion (2.18) can be reproduced. In addition, it's straightforward to confirm that Eq. (2.26) coincides with (2.19).

Now, solving for $\Lambda_{\mu\nu}$ from Eq. (2.25) and plugging it into the action (2.21) yields

$$S = \int d^4x\sqrt{-g}\left[\frac{M_P^2}{2}R + \lambda(G_{ab}\partial^\mu\phi^a\partial_\mu\phi^b + \Omega) + \mathcal{L}_m\right], \tag{2.27}$$

which is the same as action (2.13) with $\mathcal{L} = -V(\phi^a)$ and $\lambda \equiv \Omega^{-1}\Lambda$.

It is worth mentioning that the action (2.13) reduces to that of [7] when G_{ab} is constant. Now, by rescaling the fields via $\phi^a \to \sqrt{\Omega}\phi^a$, we can absorb the effects of the constant Ω into the Lagrange multiplier. Therefore, from now on we set $\Omega = 1$ without a loss of generality.

Note that in Ref. [7] the shift symmetry for two scalar fields in the absence of the potential function was imposed so the metric G_{ab} was diagonal with constant elements. However, here we work in a curved field space manifold with the metric $G_{ab}(\phi^c)$ so the shift symmetry is explicitly broken. Furthermore, in the absence of shift symmetry, we have allowed for the potential term $V(\phi^a)$ as well.

III. MULTIFIELD MIMETIC COSMOLOGY

The goal of this section is to write down the background equations and the quadratic action of cosmological perturbations in a covariance form. The value of the scalar fields $\phi^a(x^\mu)$ at a given location in spacetime consists of the homogeneous background value, ϕ_0^a, and the gauge dependent fluctuations, $\delta\phi^a$. The fluctuations $\delta\phi^a$ describe a finite coordinate displacement from the classical trajectory so they are not covariant. This motivates the construction of a vector field Q^a in order to write down the field fluctuations in a covariant form.

The two points like $\phi_0^a(t)$ and $\phi^a = \phi_0^a + \delta\phi^a$ are connected by a unique geodesic with respect to the field space metric G_{ab} [56,70]. This geodesic is parametrized by ε, such that $\phi^a(\varepsilon = 0) = \phi_0^a$ and $\phi^a(\varepsilon = 1) = \phi_0^a + \delta\phi$. These boundary conditions determine a unique vector Q^a, which connects the two scalar field values in such a way that $D_\varepsilon\phi^a|_{\varepsilon=0} = Q^a$ where D is the covariant derivative with respect to the field space metric G_{ab}. Therefore, one can expand $\delta\phi^a$ as a power series of Q^a as [56,70],

$$\delta\phi^a = Q^a - \frac{1}{2}\Gamma^a_{bc}Q^bQ^c + \frac{1}{6}(\Gamma^a_{de}\Gamma^e_{bc} - \Gamma^a_{bc;d})Q^bQ^cQ^d + \cdots, \tag{3.1}$$

in which Γ^a_{bc} represents the Christoffel symbol associated with the metric G_{ab}.

Note that at linear order, the field fluctuations $\delta\phi^a$ and the vector Q^a are identical but at higher orders they are different. Thus, in the covariant manner, we must write the equations in terms of Q^a. In addition to scalar fields' perturbations, we need to perturb the metric components and the Lagrange multiplier.

The cosmological background in the absence of perturbations is given by the FLRW metric

$$ds^2 = -dt^2 + a(t)^2 d\mathbf{x}^2, \tag{3.2}$$

in which $a(t)$ is the scale factor. Now denoting the components of the full metric via $g_{00} = -\mathcal{N}^2 + \beta_i\beta^i$, $g_{0i} = \beta_i$, $g_{ij} = \gamma_{ij}$, the scalar perturbation parts of the metric at linear order are defined as

$$\mathcal{N} = 1 + \alpha, \quad \beta_i = B_{,i}, \quad \gamma_{ij} = a^2 e^{2\psi}\delta_{ij} \tag{3.3}$$

where in spatially flat gauge we take $\psi = 0$ and therefore $\gamma_{ij} = a^2\delta_{ij}$. Furthermore, $\mathcal{N}$ is the lapse function while β_i is the shift vector

In addition, there is the scalar perturbation $\lambda = \lambda_0(t) + \delta\lambda(t, \vec{x})$ for the Lagrange multiplier. Substituting these perturbations back into the action (2.13) and solving for the constraint equations, we obtain the quadratic action for the field fluctuations Q^a.

A. Background solutions

In order to derive the background equations of motion, we expand the action (2.13) up to the linear order of scalar perturbations (3.3) and (3.1) by performing the analysis in spatially flat gauge. Substituting these solutions back into the action (2.13), the first order action becomes

$$S_1 = \mathcal{V}\int \mathrm{d}t\, a^3 [(G_{ab}(6H\lambda_0 + 2\dot{\lambda}_0)\dot{\phi}_0^a - V_b + 2G_{ab}\lambda_0 D_t\dot{\phi}_0^a)Q^b + (-V + 3M_P^2H^2 + \lambda_0(1 + G_{bc}\dot{\phi}_0^b\dot{\phi}_0^c)\alpha + \delta\lambda(1 - G_{bc}\dot{\phi}_0^b\dot{\phi}_0^c))], \tag{3.4}$$

where $V^b \equiv G^{ab}\partial_b V$ and $\mathcal{V} = \int \mathrm{d}^3x$ is the spatial volume, which will be assumed to be large enough but finite.

Clearly, the variation with respect to Lagrangian multiplier perturbation mode $\delta\lambda$ gives us the mimetic constraint at the background level, i.e.,

$$G_{ab}\dot{\phi}_0^a\dot{\phi}_0^b = 1 \quad \text{or} \quad G_{ab}D_t\dot{\phi}_0^a\dot{\phi}_0^b = 0, \tag{3.5}$$

in which the convenient derivative is given by

$$D_tX^a = \dot{X}^a + \Gamma^a_{bc}X^b\dot{\phi}_0^c. \tag{3.6}$$

Here we have used $D_tG_{ab} = 0$, which follows from the definition of the covariant differentiation.

Now, we can derive additional equations of motion by varying with respect to the field fluctuation Q^a and α. Taking the variation of (3.4) with respect to Q^b, we arrive at

$$\lambda_0 D_t\dot{\phi}_0^a = \frac{V^a}{2} - (3H\lambda_0 + \dot{\lambda}_0)\dot{\phi}_0^a, \tag{3.7}$$

in which $H = \dot{a}(t)/a(t)$ is the Hubble expansion rate.

After contracting both sides of the above equation by $\dot{\phi}_0^b$ and using Eq. (3.5), we obtain

$$\dot{\lambda}_0 = \frac{1}{2}(V_a\dot{\phi}_0^a - 6H\lambda_0). \tag{3.8}$$

The other equation comes from the variation of the action with respect to α, yielding,

$$3M_P^2H^2 + 2\lambda_0 = V. \tag{3.9}$$

As we take time derivative from both sides of the above equation and compare with Eq. (3.8), we can immediately find

$$\lambda_0 = M_P^2\dot{H}. \tag{3.10}$$

Now combining Eqs. (3.10) and (3.9) one obtains the Friedmann equation,

$$M_P^2(3H^2 + 2\dot{H}) = V. \tag{3.11}$$

In the absence of the potential function, using Eqs. (3.10), (3.11), and (3.8), one finds $\lambda_0 \sim 1/a^3$ and $H(t) = 2/(3t)$ (see Fig. 1 for an example).

On the other hand, by varying the action (2.13) with respect to the metric $g_{\mu\nu}$, the effective energy momentum tensor is given by

$$T^\mu_\nu = -V\delta^\mu_\nu - 2\lambda G_{ab}\partial^\mu\phi^a\partial_\nu\phi^b. \tag{3.12}$$

Correspondingly, one can read the energy density and the pressure as $\rho = T^0_0$ and $P = \frac{1}{3}T^i_i$.

For the case with no potential, $V = 0$, using the mimetic constraint (3.5) and $\lambda_0 \sim 1/a^3$ we obtain $\rho = 2\lambda_0 \propto a^{-3}$ and $P = 0$. Therefore, similar to the standard single field mimetic theory [1], the multifield generalization of the setup mimics the role of dark matter.[3]

In order to understand the effect of the mimetic constraint (3.5) on the fields trajectory in the curved field space, let us consider, for example, an interesting two-field model proposed in [71] for axion inflation. In this model, the axion field ϕ^2 is characterized as the phase of a complex scalar field Φ ($\Phi = \phi^1 e^{i\phi^2}$) in a canonical $U(1)$ symmetry-breaking model in which the complex scalar field Φ has a nonminimal coupling to gravity in the Jordan frame, i.e., $f(\Phi)R$. Moreover, the radial component ϕ^1, as a second scalar field, plays the role of the order parameter of the symmetry breaking. The nonminimal coupling depends only on the radial field, i.e., $f = f(\phi^1)$, and the kinetic terms of these polar coordinates have the flat field space metric in Jordan frame.

On the other hand, going to the Einstein frame by performing a conformal transformation of the spacetime metric such as $g_{\mu\nu} = 2f(\phi^1)/M_p^2\tilde{g}_{\mu\nu}$, the field-space metric becomes [71],

$$G_{11} = \frac{M_P^2}{2f}\left(1 + \frac{3f^2_{,\phi^1}}{f}\right), \quad G_{22} = \frac{M_P^2}{2f}(\phi^1)^2, \quad G_{12} = G_{21} = 0, \tag{3.13}$$

which describes a curved field space with the coupling f given by $f(\phi^1) = \frac{1}{2}(M^2 + \xi(\phi^1)^2)$. Moreover, the potential function takes the following form in the Einstein frame [71]

$$V(\phi^1, \phi^2) = \frac{\zeta M_P^4}{16}\frac{((\phi^1)^2 - v^2)^2}{f^2} + \frac{M_P^4\Lambda^4}{4f^2}(1 - \cos(\phi^2)). \tag{3.14}$$

Here M, ξ, ϵ_V, v, and Λ are parameters of the model. As seen, the potential function consists of two terms. The first term is related to the spontaneous symmetry breaking (Higgs) potential of the radial field and the second term comes from the nonperturbative effects that generate a potential for the axion field.

As another example, we consider a two-field model with a polar parametrization, $\phi^a = (\phi^1, \phi^2)$, with a shift symmetry through the angular direction $\phi^2 \to \phi^2 + c$ [64]. In this respect, the radial field space coordinate ϕ^1 is orthogonal to the isometry while the angular coordinate ϕ^2 is tangential to it. The simple form of a such field space in the "orbital inflation" model [64] is defined as follows:

$$G_{11} = 1, \qquad G_{22} = f(\phi^1), \qquad G_{12} = G_{21} = 0, \tag{3.15}$$

in which one chooses $f(\phi^1) = e^{2\phi^1/R_0}$ associated with a hyperbolic field metric which has the Ricci curvature $\mathbb{R} = -2/R_0^2$. In addition, for a specific model of the orbital inflation, the potential function takes the following form:

$$V(\phi^1,\phi^2) = 3\mathcal{A}\left(\phi^2 - \frac{2}{3f}\right)\left(1 + \frac{\beta}{2}(\phi^1 - \varphi)^2 + \frac{\alpha}{6}(\phi^1 - \varphi)^3\right)^2 - 2\mathcal{A}^2(\phi^2)^2\left(\beta(\phi^1 - \varphi) + \frac{\alpha}{2}(\phi^1 - \varphi)^2\right)^2. \tag{3.16}$$

Notice that inflation happens at constant radius $\phi^1 = \varphi$ in the orbital inflation setup, but here we only consider this model as a toy model with free parameters $\mathcal{A}$, α, β, R_0, and φ.

In Fig. 1, we have presented the evolution of $\lambda_0(t)$ in the field space for the above two metrics for both cases $V = 0$ and $V \neq 0$. The left panel refers to the axion inflation example with the metric (3.13), while the right panel corresponds to the case of orbital inflation with the metric (3.15) and potential (3.16). The red solid and blue dashed curves represent the cases $V = 0$ and $V \neq 0$, respectively. As we see for the case $V = 0$, the curve for λ_0 (or equivalently ρ) scales like $1/a^3$, which describes the energy density in matter-dominated era, whereas one observes a deviation form $1/a^3$ when $V \neq 0$. For the case of axion inflation, the numerical parameters are $\phi^1_0 = 0.5$, $\phi^2_0 = 0.97\pi$, $\dot{\phi}^1_0 = -0.025$, $M = 10^{-2}$, $\lambda_0(0) = -0.375$, $\xi = 1$, $v = \sqrt{\frac{99}{100}}$, $\zeta = 0.07$, $\Lambda = 2.74 \times 10^{-3}$ in units of M_P. In the case of orbital inflation, we choose $\phi^1_0 = 0.5$, $\phi^2_0 = 0.1$, $\dot{\phi}^1_0 = 0$, $R_0 = 50$, $\beta = 0.1$, $\alpha = 0.01$, $\varphi = 1$, $\mathcal{A} = 10^{-4}$.

[3]We comment that by expanding the mimetic cosmology to models containing multiple gauge fields with a certain mimetic constraint imposed on the gauge field strength tensor, the Maxwell term can play the role of the cosmological constant yielding to a de Sitter–like spacetime [19,20].

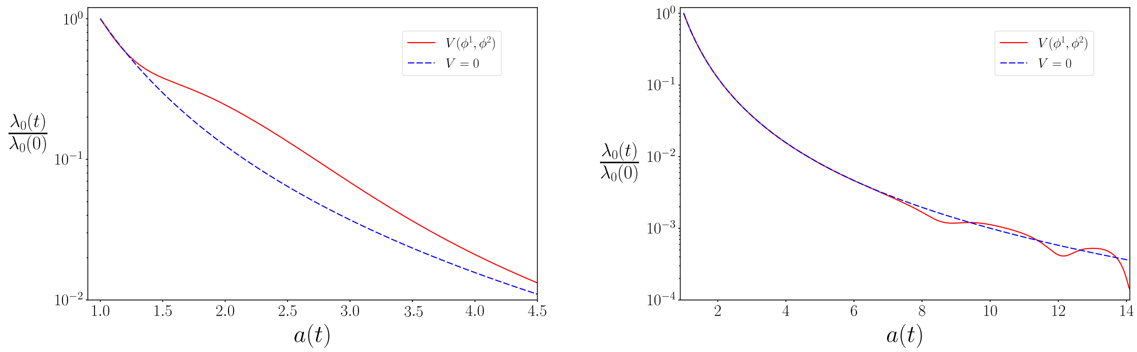

FIG. 1. The evolution of the Lagrange multiplier for two different cases $V \neq 0$ (red solid curve) and $V = 0$ (blue dashed curve). Left panel: the axion inflation example with the metric (3.13) and potential (3.14). Right panel: the orbital inflation example with the metric (3.15) and potential (3.16). The $V = 0$ case corresponds to a matter dominated Universe in which $\lambda(t) \propto a(t)^{-3}$ or equivalently $\rho \propto a^{-3}$ and $H = 2/(3t)$.

In addition, Fig. 2 shows the background trajectory in the field space for the above two examples. As illustrated in first two rows of Fig. 2, one can observe sudden turns in the trajectory where the potential function V is nonzero.

B. Quadratic action

In this part, we present the cosmological perturbations analysis in the spatially flat gauge. By expanding the action (2.13) up to the second order of scalar perturbations (3.3) and (3.1), the quadratic action takes the following form:

$$S^2 = \int \mathrm{d}t\, \mathrm{d}^3x a^3 \bigg[M_P^2 \epsilon H^2 G_{bc} D_t Q^b D_t Q^c - \left(\frac{1}{2} V_{bc} + M_P^2 \epsilon H^2 \mathbb{R}_{bdcf} \dot{\phi}_0^d \dot{\phi}_0^f \right) Q^b Q^c + 2\delta\lambda(\alpha - D_t Q_b \dot{\phi}_0^b) - \alpha(V_b Q^b + 3M_P^2 H^2 \alpha - M_P^2 \epsilon H^2 \alpha + 2\epsilon H^2 D_t Q_b \dot{\phi}_0^b) - 2M_P^2 H(\alpha - \epsilon H Q_b \dot{\phi}_0^b) \partial_i \partial^i B - \frac{M_P^2}{a^2} \epsilon H^2 G_{ab} \partial_i Q^b \partial_i Q^c \bigg], \tag{3.17}$$

where $V_{ab} = V_{;ab}$,

$$\mathbb{R}^a_{bd,c} \equiv \Gamma^a_{bd,c} - \Gamma^a_{bc,d} + \Gamma^a_{ce}\Gamma^c_{bd} - \Gamma^a_{de}\Gamma^e_{bc} \tag{3.18}$$

is the Riemann tensor associated with the curved field space, and ϵ is the "slow-roll" parameter that is defined by $\epsilon \equiv -\dot{H}/H^2$.

From the above quadratic action, we see that the quadratic Lagrangian is linear in terms of the nondynamical mode B, from which its equation of motion yields

$$\alpha = \epsilon H Q_b \dot{\phi}_0^b. \tag{3.19}$$

It is worth mentioning that the linearity of the B mode in the quadratic action causes the adiabatic perturbation to be nondynamical in the two-field mimetic example (see below).

Plugging the relation (3.19) in action (3.17), the reduced action takes the following form

$$S^2 = \int d^3x dt\, a^3 \bigg[M_P^2 \epsilon H^2 G_{bc} D_t Q^b D_t Q^c - 2M_P^2 \epsilon^2 H^3 Q_b D_t Q_c \dot{\phi}_0^b \dot{\phi}_0^c - M_{bc}^2 Q^b Q^c - \frac{M_P^2}{a^2} \epsilon H^2 G_{bc} \partial_i Q^b \partial^i Q^c + 2\delta\lambda(\epsilon H Q_b \dot{\phi}_0^b - D_t Q_b \dot{\phi}_0^b) \bigg], \tag{3.20}$$

where the effective mass matrix is defined via

$$M_{ab} \equiv \frac{V_{ab}}{2} + \frac{1}{2} \epsilon H (V_a \dot{\phi}_{0b} + V_b \dot{\phi}_{0a}) + M_P^2 \epsilon^2 H^4 (3 - \epsilon) \dot{\phi}_{0a} \dot{\phi}_{0b} + M_P^2 \epsilon H^2 \mathbb{R}_{acbd} \dot{\phi}_0^c \dot{\phi}_0^d. \tag{3.21}$$

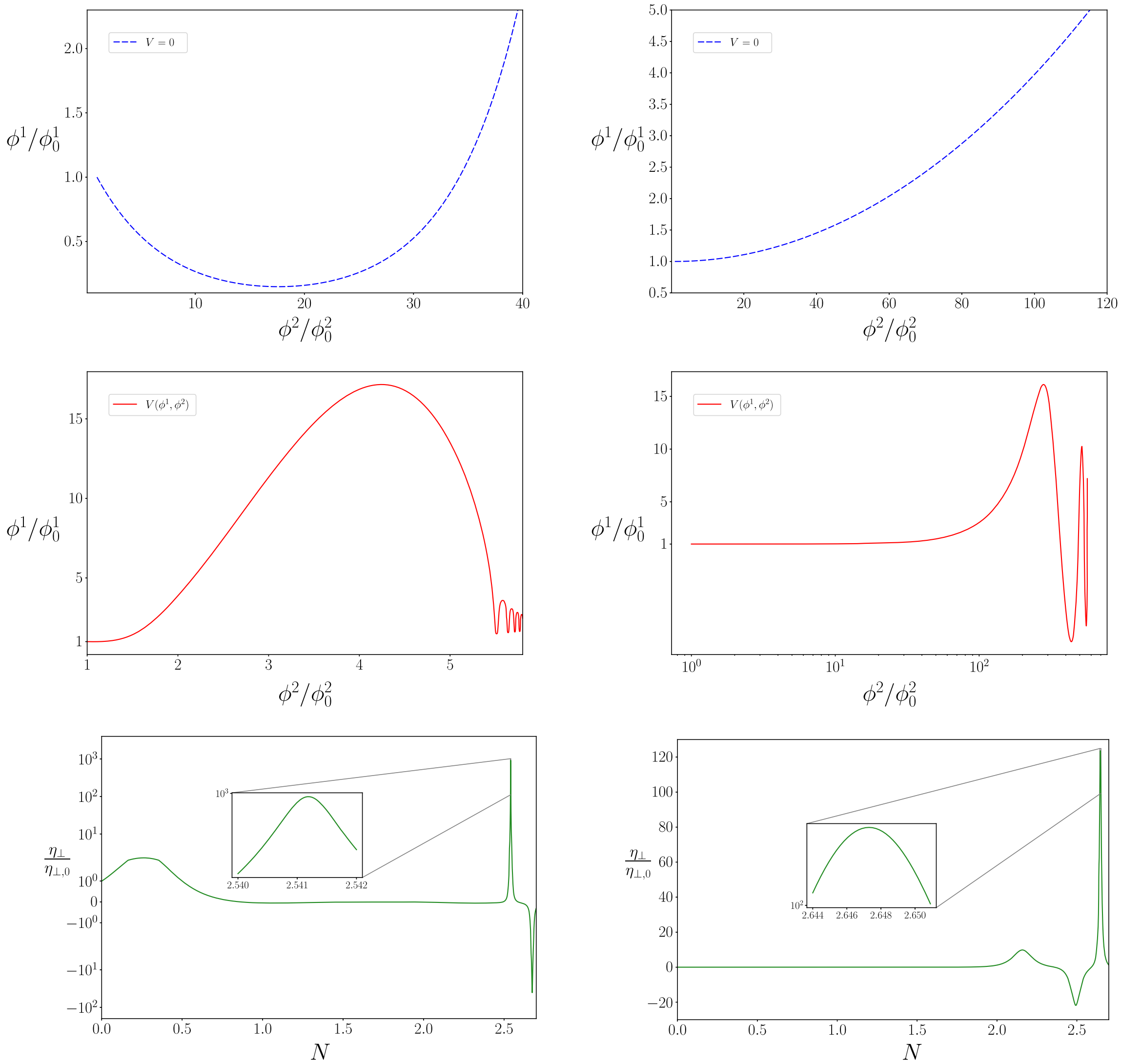

FIG. 2. Illustration of the trajectory in field space and the evolution of the turning rate $\eta_\perp$. Left panels: the axion inflation example with the metric (3.13) and potential (3.14). Right panels: the orbital inflation example with the metric (3.15) and potential (3.16). The parameters are the same as those used in Fig. 1. The oscillatory behavior of the trajectory (or changing sign in the tuning rate $\eta_\perp$) is due to the centrifugal force of the potential. This behavior can also be seen from the turning rate parameter $\eta_\perp$ plotted in Fig. 4. Although the trajectory for the case $V = 0$ is curved, the rate of the turn is zero.

Finally, taking the variation of the above action with respect to $\delta\lambda$ yields the following relation

$$D_t Q_b \dot{\phi}_0^b = \epsilon H Q_b \dot{\phi}_0^b. \tag{3.22}$$

Our analysis so far was general, valid for any number of fields. In the rest of this section we restrict ourselves to the case of two-dimensional field space. This is because we will work in a new coordinate in the field space where the perturbations are decomposed into the parallel to the background trajectory and perpendicular to it. While this decomposition is valid for field space of any dimension, but its geometric visualization is more simple in the case of 2D field manifold.

In a 2D field space with the coordinate $\phi_0^a(t) = (\phi_0^1(t), \phi_0^2(t))$, any trajectory defined in this space is parametrized by cosmic time t. To characterize this curve, it is useful to construct a set of orthogonal unit vectors T^a and N^a such that at a given time t, $T^a(t)$ is tangent to the path while $N^a(t)$ is normal to it [56,70]. In Fig. 3 we have illustrated a schematic plot of the evolution of the this set of orthonormal vectors along the background trajectory in the field space. This set of vectors is defined as

$$T^a = \frac{\dot{\phi}_0^a}{\dot{\phi}_0}, \tag{3.23}$$

$$N_a = (\mathrm{sgn}(\pm 1) G)^{1/2} \epsilon_{ab} T^b, \tag{3.24}$$

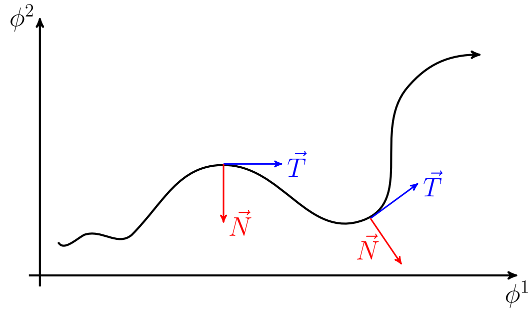

FIG. 3. A schematic view of the evolution of the tangent vector T^a and normal vector N^a along the field space trajectory.

where $\dot{\phi}_0^2 = G_{ab}\dot{\phi}_0^a\dot{\phi}_0^b$, which equals to one according to (3.5). Moreover, G is the determinant of the metric G_{ab}, the signum function $\mathrm{sgn}(\pm 1)$ determines the signature of G_{ab}, for instance, $\mathrm{sgn}(-1)$ is for Lorentzian signature, whereas $\mathrm{sgn}(+1)$ is chosen for the Euclidean signature. In addition, ϵ_{ab} is the two dimensional Levi-Civita symbol with $\epsilon_{11} = \epsilon_{22} = 0$ and $\epsilon_{12} = -\epsilon_{21} = 1$. These definitions satisfy the following conditions: $T_aT^a = 1$, $N_aN^a = \mathrm{sgn}(\pm 1)$ and $T^aN_a = 0$ [56,70]. Notice that the mimetic constraint (3.5) in term of this set of vectors can be written as $G_{ab}\dot{\phi}_0^a\dot{\phi}_0^b = T_aT^a = 1$.

These two unit orthogonal vectors may be used to project the scalar field equation of motion (3.7) along these directions. Projecting along T^a, we obtain Eq. (3.9), whereas by projecting along N^a one obtains the relation

$$D_t\dot{\phi}_0^a = \frac{DT^a}{dt} = \frac{V_N}{2\lambda_0}N^a, \tag{3.25}$$

where $V_N \equiv N^a\partial_a V$. Clearly, this relation satisfies the mimetic constraint (3.5). Now, let us define the second "slow-roll" parameter η^a as

$$\eta^a \equiv -\frac{D\dot{\phi}_0^a}{dt} = -\eta_\perp N^a, \tag{3.26}$$

with its normal component given by $\eta_\perp = V_N/2\lambda_0$. Combining this relation with (3.25), we deduce the following relations:

$$\frac{DT^a}{dt} = \eta_\perp N^a, \tag{3.27}$$

$$\frac{DN^a}{dt} = -\eta_\perp T^a. \tag{3.28}$$

Therefore, if $\eta_\perp = 0$, then the vectors T^a and N^a remain covariantly constant with respect to D_t [but not with respect to ∂_t, see the definition (3.6)] along the path. If $\eta_\perp > 0$, then the path turns to the left, whereas if $\eta_\perp < 0$, then the turn is towards the right. The value of $\eta_\perp$ therefore indicates how quickly the angle determining the orientation of T^a varies in time. Denoting this angle by θ we may therefore do the identification[4]

$$\dot{\theta} \equiv \eta_\perp. \tag{3.29}$$

In the last row of Fig. 2 and in Fig. 4, we have plotted the evolution of $\eta_\perp$ for the case $V \neq 0$ with respect to the number of e-folds N and fields ϕ^1 and ϕ^2, respectively. As expected, the sudden turn in the field trajectory in Fig. 2 is translated into the change of the sign of $\eta_\perp$ in Fig. 2 and to moving to the left or right in Fig. 4.

For the two-field case, the parallel and normal perturbations with respect to the background trajectory are given, respectively, by

$$u^T \equiv Q^T \equiv T_aQ^a, \tag{3.30}$$

$$u^N \equiv Q^N \equiv N_aQ^a. \tag{3.31}$$

In this transformation u^T corresponds to the perturbations parallel to the background trajectory while u^N corresponds to perturbations normal to the trajectory which represents the entropy perturbations, i.e., the nonadiabatic mode [56,70,72].

By using the above representations and replacing $\dot{\phi}_0^c$ and $D_t\dot{\phi}_0^c$ by the tangent and normal vectors T^c and N^c according to Eqs. (3.23) and (3.25), the quadratic action (3.20), after straightforward manipulations, reads

$$S^2 = \int d^3xdta^3M_P^2\epsilon H^2\Bigg[\mathcal{L}_{u_N} + \mathcal{L}_{u_T} + 2\mathrm{sgn}(\pm 1)\dot{\theta}u_T\dot{u}_N - 2\dot{\theta}u_N\dot{u}_T - 2\left(\frac{M_{NT}^2}{M_P^2\epsilon H^2} - \epsilon H\dot{\theta}\right)u_Tu_N + \frac{2}{M_P^2H}\delta\lambda\left(u_T - \frac{\dot{u}_T}{\epsilon H} + \frac{1}{\epsilon H}\dot{\theta}u_N\right)\Bigg], \tag{3.32}$$

with

$$\mathcal{L}_{u_N} \equiv \mathrm{sgn}(\pm 1)\left(\dot{u}_N^2 - \frac{1}{a^2}(\partial u_N)^2\right) + \left(\dot{\theta}^2 - \frac{M_{NN}^2}{M_P^2\epsilon H^2}\right)u_N^2, \tag{3.33}$$

[4]Utilizing this definition, we see that the ratio of curvature κ_R characterizing the turning trajectory is defined as [56,70] $\kappa_R^{-1} \equiv |\dot{\theta}|$.

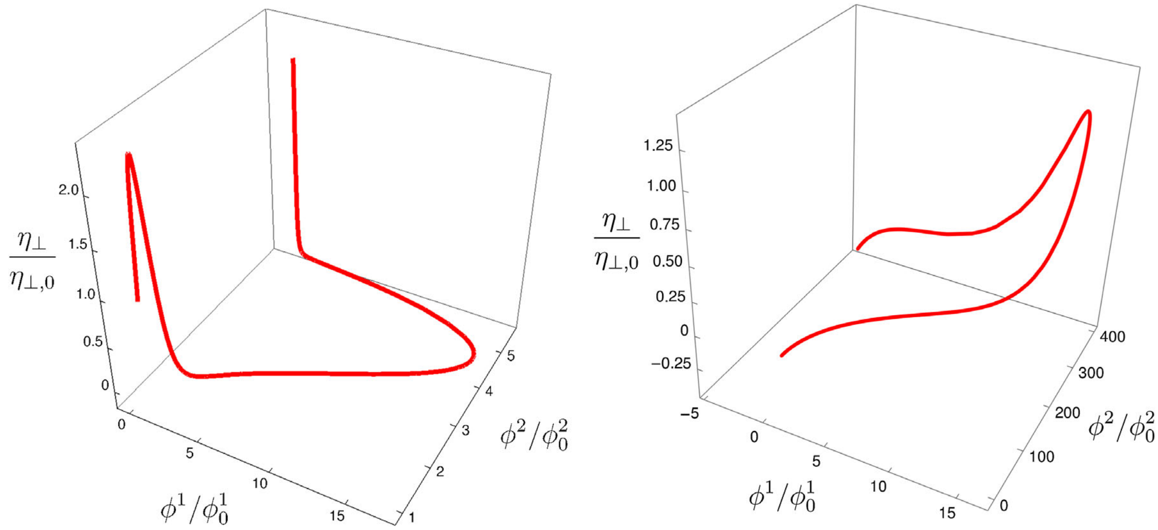

FIG. 4. The figure shows the evolution of turning rate $\eta_\perp$ in terms of the mimetic fields ϕ^1 and ϕ^2. Left panel: the axion inflation example with the metric (3.13) and potential (3.14). Right panel: the orbital inflation example with the metric (3.15) and potential (3.16). The parameters are the same as those used in Fig. 1. This plot is consistent with Fig. 2 meaning that the turning toward left (right) in the field space indicates that $\eta_\perp$ increases (decreases).

and

$$\mathcal{L}_{u_T} \equiv \dot{u}_T^2 - \frac{1}{a^2}(\partial u_T)^2 - 2\epsilon H u_T \dot{u}_T + \left(\mathrm{sgn}(\pm1)\dot{\theta}^2 - \frac{M_{TT}^2}{M_P^2 \epsilon H^2}\right) u_T^2, \qquad (3.34)$$

where $\eta_H \equiv \dot{\epsilon}/H\epsilon$ and the symmetric matrix M_{IJ} elements are given by

$$M_{NN}^2 \equiv N^a N^b M_{ab}^2 = \frac{1}{2}(V_{NN} - \mathrm{sgn}(\pm1)\epsilon H^2 \mathbb{R}), \qquad (3.35)$$

$$M_{TT}^2 \equiv T^a T^b M_{ab}^2 = \frac{V_{TT}}{2} + \epsilon H (V_T + M_P^2 \epsilon H^3 (3-\epsilon)), \qquad (3.36)$$

$$M_{NT}^2 \equiv M_{TN}^2 = T^a N^b M_{ab}^2 = \frac{1}{2}(V_{NT} + \epsilon H V_N), \qquad (3.37)$$

where $V_{NT} \equiv N^a T^b V_{;ab}$, $V_{NN} \equiv N^a N^b V_{;ab}$, and $V_{TT} \equiv T^a T^b V_{;ab}$. In particular, note the effect of the Ricci scalar $\mathbb{R}$ associated with the field space manifold. Since we consider a 2D field space here, the Riemann tensor can be expressed in the terms of the Ricci scalar $\mathbb{R}$ as

$$\mathbb{R}_{abcd} = \frac{1}{2}\mathbb{R}(G_{ac}G_{bd} - G_{ad}G_{cb}). \qquad (3.38)$$

Finally, the equation of motion for $\delta\lambda$ then yields

$$\dot{u}_T = \epsilon H u_T + \dot{\theta} u_N. \qquad (3.39)$$

Substituting the above result into Eq. (3.32), we arrive at our final reduced quadratic action

$$S^2 = \int d^3x dt a^3 M_P^2 \epsilon H^2 \Big\{ \mathrm{sgn}(\pm1)\left(\dot{u}_N^2 - \frac{1}{a^2}(\partial u_N)^2\right) - \frac{M_{NN}^2}{M_P^2 \epsilon H^2} u_N^2 - \frac{1}{a^2}(\partial u_T)^2 + \left(\mathrm{sgn}(\pm1)\dot{\theta}^2 - \epsilon^2 H^2 - \frac{M_{TT}^2}{M_P^2 \epsilon H^2}\right) u_T^2 + 2\mathrm{sgn}(\pm1)\dot{\theta} u_T \dot{u}_N - 2\frac{M_{NT}^2}{\epsilon H^2} u_N u_T \Big\}. \qquad (3.40)$$

From the above action, it is clear that the perturbation mode perpendicular to background trajectory, u_N, is excited while the perturbation mode tangential to background trajectory, u_T, does not propagate. In other words, the entropy mode propagates with the speed of unity, whereas the sound speed for the adiabatic mode is zero. This is consistent with the fact that the mimetic background describes a fluid with no pressure. In addition, whether the entropy perturbation is free from the gradient as well as ghost instabilities directly depends on the signature of the metric, i.e., $\mathrm{sgn}(\pm1)$. In the case of the field space with an Euclidean signature [$\mathrm{sgn}(+1) = 1$], the entropy mode is healthy, whereas in the case of the Lorentzian manifold with $\mathrm{sgn}(-1) = -1$, the entropy perturbation is pathological. As one turns off the potential function V in our setup and consider the flat metric, i.e., $G_{ab} = \delta_{ab}$ with an Euclidean signature, this action converts to Eq. (53) in [7] with the healthy entropy perturbation. However, when one considers $G_{ab} = \mathrm{diag}(1, -1)$, the entropy mode always suffers from the ghost and gradient instabilities [23]. In Appendix B we confirm these conclusions in the comoving gauge as well.

Now let us check the number of degrees of freedom (DOFs) of the setup at the linear cosmological perturbation level by performing the Hamiltonian analysis of the quadratic action (3.32). It is evident that the time derivative of $\delta\lambda$ does not appear in the action (3.32) so one has the primary constraint $\Xi_1 \equiv \Pi_{\delta\lambda} = 0$, where $\Pi_{\delta\lambda}$ is the conjugate momentum associated with $\delta\lambda$. After imposing this primary constraint, the total Hamiltonian is given by

$$H_T = \int d^3x(\Pi_{u_T}\dot{u}_T + \Pi_{u_N}\dot{u}_N - \mathcal{L} + v\Xi_1), \qquad (3.41)$$

where v is the Lagrangian multiplier. By constructing the conjugate momentum $\Pi_{u_T} = \partial\mathcal{L}/\partial\dot{u}_T$ and $\Pi_{u_N} = \partial\mathcal{L}/\partial\dot{u}_N$ from the quadratic action (3.32), the total Hamiltonian in the Fourier space is written as

$$H_T = \int dx^3 \bigg[\frac{\Pi_{u_N}^2}{4\mathrm{sgn}(\pm1)a^3M_P^2\epsilon H^2} + (\mathrm{sgn}(\pm1)a\epsilon H^2k^2 + a^3M_{NN}^2)u_N^2 + \frac{\Pi_{u_T}^2}{4a^3M_P^2\epsilon H^2} + M_P^2\epsilon H^2\left(ak^2 + a^3\epsilon^2H^2 + a^3\frac{M_{TT}^2}{\epsilon H^2}\right)u_T^2 + \frac{\delta\lambda}{M_P^2\epsilon H^2}(\Pi_{u_T} + a^3\delta\lambda) + 2a^3M_{NT}^2u_Nu_T + \epsilon H\Pi_{u_T}u_T + \dot{\theta}(\Pi_{u_T}u_N - \Pi_{u_N}u_T) + v\Xi_1\bigg]. \qquad (3.42)$$

Note that because we work in the Fourier space, all coordinate and momentum variables are only functions of time and the wave number k in which, for simplicity, their dependence on k are dropped.

In order to derive the secondary constraint, we should check the time evolution of the primary constraint Ξ_1, which amounts to examine the consistency relation. Beginning with Ξ_1, one obtains the following constraint:

$$\Xi_2 \equiv \{\Xi_1, H_T\} = -\frac{1}{M_P^2\epsilon H^2}(\Pi_{u_T} + 2a^3\delta\lambda) \approx 0. \qquad (3.43)$$

The above constraint can be solved for $\delta\lambda$, yielding

$$\delta\lambda = -\frac{\Pi_{u_T}}{2a^3}. \qquad (3.44)$$

The next consistency relation gives

$$\begin{aligned}\Xi_3 &\equiv \{\Xi_2, H_T\} \\ &= \frac{1}{M_P^2\epsilon H^2}(-2a^3v - \dot{\theta}\Pi_{u_N} + \epsilon\Pi_{u_T} + 2a^3M_{NT}^2 + 2a^3M_{TT}^2) \\ &\quad + 2(ak^2 + a^3\epsilon^2H^2)u_T \approx 0,\end{aligned} \qquad (3.45)$$

which determines the Lagrange multiplier v as a function of the phase space variables and thus the chain of constraints for primary constraint Ξ ends here. More precisely, both constraints Ξ_1 and Ξ_2 are second class constraints and therefore the physical number of DOFs is $(6-2)/2 = 2$. Together with two tensor modes, the total DOFs of our two-field setup is four. This is confirmed in next section where we present the full nonlinear Hamiltonian analysis. In spite of the fact that the adiabatic mode does not propagate at the linear perturbation level, it contributes to the physical DOFs of the model. The same result has been reported in [23] for the flat two-field setup.

As seen, the adiabatic mode u_T does not propagate in 2D field space at linear order in perturbation. This is similar to the simple single field mimetic model where the curvature perturbation was nonpropagating at the linear order. To remedy this issue, in the case of single field mimetic setup, higher derivative terms such as $(\Box\phi)^2$ were added to the theory yielding a nonzero sound speed for the curvature perturbations. Motivated by this fact, we may also consider adding higher derivative terms to our action. First consider the term

$$Y = X_{ab}X^{ab} = G_{ad}G_{bc}X^{dc}X^{ab}, \qquad (3.46)$$

where $X^{ab} = \partial^\mu\phi^a\partial_\mu\phi^b$.[5] This term is linear with respect to the nondynamical mode B. In order to prove it let us write down X^{ab} by using ADM variables as

$$X^{ab} = -\frac{1}{\mathcal{N}^2}(\dot{\phi}^a - \beta^k\partial_k\phi^a)(\dot{\phi}^b - \beta^k\partial_k\phi^b) + \gamma^{kl}\partial_k\phi^a\partial_l\phi^b. \qquad (3.47)$$

By expanding the above relation up to the second order of scalar perturbations, we arrive at

$$\begin{aligned}X^{ab} = &-\dot{\phi}_0^a\dot{\phi}_0^b + 2\alpha\dot{\phi}_0^a\dot{\phi}_0^b - (\dot{\phi}_0^a\dot{Q}^b + \dot{\phi}_0^b\dot{Q}^a) \\ &- 3\alpha^2\dot{\phi}_0^a\dot{\phi}_0^b + 2\alpha(\dot{\phi}_0^a\dot{Q}^b + \dot{\phi}_0^b\dot{Q}^a) \\ &- \dot{Q}^a\dot{Q}^b + \partial^kB(\partial_kQ^a\dot{\phi}_0^b + \partial_kQ^b\dot{\phi}_0^a) \\ &+ a^2\delta^{kl}\partial_kQ^a\partial_lQ^b.\end{aligned} \qquad (3.48)$$

[5]Note that the term $G_{ab}\Box\phi^a\Box\phi^b$ is not covariant in field space nor in spacetime.

Clearly, the scalar Y is linear with respect to the nondynamical mode B up to the second order. This confirms that the adiabatic mode does not propagate in our model just by adding the Y term to the action. Therefore, one may consider to couple nonminimally a function of Y term to the spacetime Ricci scalar R. Since the Ricci scalar is linear with respect to B, adding $f(Y)R$ to the action can not generate any nonlinear contributions of B as well. After eliminating nondynamical modes in the corresponding quadratic action, Eq. (3.22) is still satisfied and it prevents the adiabatic mode u_T to propagate.

Similar to the single field mimetic scenario, let us now consider box terms such as

$$(\Box L)^2, \tag{3.49}$$

where $L^2 \equiv G_{ab}\phi^a\phi^b$ describes the length in the field space. This box term is defined as

$$\Box L = \frac{1}{\sqrt{-g}}\partial_\mu(\sqrt{-g}g^{\mu\nu}\partial_\nu L) \supseteq \partial_k g^{k0}\dot{L} + \ddot{L}. \tag{3.50}$$

Correspondingly, its contribution to the quadratic action yields

$$\begin{aligned} S^2 &\supseteq \int dx^3 dt (\Box L)^2 \\ &\supseteq \int d^3x dt ((\partial_k\partial^k B)^2 \dot{\bar{L}}^2 + \delta\ddot{L}^2), \end{aligned} \tag{3.51}$$

where $\bar{L} = G_{ab}\phi_0^a\phi_0^b$ and $\delta L = L - \bar{L}$. It is obvious that the quadratic action contains not only the gradient term $(\partial^2 B)^2$, but also the higher derivative term $\delta\ddot{L}$ which is the source of the Ostrogradsky ghost. As mentioned earlier, incorporating a nonlinear term for the B mode in the quadratic action modifies the relation (3.22), causing the adiabatic modes u_T to propagate. However, this comes with the price that both entropy and adiabatic modes develop Ostrogradsky-type ghost. This kind of ghost can be removed by applying explicit combinations of higher derivative terms used in Horndeski theories [73] and the higher derivative interactions coupled to gravity [74] as for example employed in single field mimetic setup [52–54].

IV. NONLINEAR HAMILTONIAN ANALYSIS

In this section we present the full nonlinear Hamiltonian analysis of the system to count the correct number of DOFs. This is motivated in part from the fact that the adiabatic mode is not propagating at the linear order of equation of motion so one may wrongly conclude that there is only one scalar degree of freedom. Although this issue is addressed in previous section using the quadratic Hamiltonian analysis, but here we confirm it employing full nonlinear perturbation analysis.

We perform the nonlinear Hamiltonian analysis using the ADM decomposition [66]. In fact, the ADM decomposition is used to characterize the nature of gravity as a constrained system. In accord with the ADM decomposition, the metric components of spacetime take the following form:

$$\begin{aligned} &g_{00} = -\mathcal{N}^2 + \beta_i\beta^i, \qquad g_{0i} = \beta_i, \qquad g_{ij} = \gamma_{ij}, \\ &g^{00} = -\frac{1}{\mathcal{N}^2}, \qquad g^{0i} = \frac{\beta^i}{\mathcal{N}^2}, \qquad g^{ij} = \gamma^{ij} - \frac{\beta^i\beta^j}{\mathcal{N}^2}, \end{aligned} \tag{4.1}$$

whereas before $\mathcal{N}$ is the lapse function and β^i is the shift vector. The spatial component γ_{ij} is defined as a metric on the three-dimensional spatial hypersurface embedded in the full spacetime.

In the ADM framework, the action (2.13) can be written as

$$S = S_G + S_M, \tag{4.2}$$

where S_G is associated to the pure gravity part, i.e.,

$$S_G = \int d^4x\sqrt{\gamma}\mathcal{N}\frac{M_P^2}{2}(R^{(3)} + K_{ij}K^{ij} - K^2), \tag{4.3}$$

where $R^{(3)}$ is the curvature of three-dimensional spatial hypersurface, constructed from γ_{ij}. Moreover, K_{ij} is the extrinsic curvature defined as

$$K_{ij} = \frac{1}{2\mathcal{N}}(\partial_t\gamma_{ij} - \beta_{i;j} - \beta_{j;i}), \qquad K \equiv K^i{}_i, \tag{4.4}$$

with the covariant derivative being calculated with respect to γ_{ij}.

On the other hand, one can write the matter part of the action as

$$S_M = \int d^4x\sqrt{\gamma}\mathcal{N}\left\{\lambda\left[-\frac{G_{ab}}{\mathcal{N}^2}(\partial_t\phi^a - \beta^k\partial_k\phi^a)(\partial_t\phi^b - \beta^l\partial_l\phi^b) + G_{ab}\gamma^{kl}\partial_k\phi^a\partial_l\phi^b + 1\right] - V\right\}.$$

Note that these actions do not depend upon the time derivative of $\mathcal{N}$, β^i, and λ. It means that these quantities are not dynamical variables. Consequently the dynamical variables are γ_{ij} and ϕ^a. The momentum canonically conjugate to γ_{ij} and ϕ^a, respectively, are

$$\Pi^{ij} = \frac{\delta S_G}{\delta \partial_t \gamma_{ij}} = \frac{M_P^2}{2}\sqrt{\gamma}(K^{ij} - \gamma^{ij}K), \tag{4.5}$$

$$\Pi_a = \frac{\delta S_M}{\delta \partial_t \phi^a} = -\frac{2\sqrt{\gamma}}{\mathcal{N}}\lambda G_{ab}(\partial_t\phi^b - \beta^i\partial_i\phi^b). \tag{4.6}$$

Plugging the above expression of the conjugate momenta in the action (4.3), the total mimetic action can be expressed as

$$S = \int d^4x[\Pi^{ij}\partial_t\gamma_{ij} + \Pi_a\partial_t\phi^a - \mathcal{N}(\mathcal{H}_G + \mathcal{H}_M) - \beta^i(\mathcal{H}_{Gi} + \mathcal{H}_{Mi})], \tag{4.7}$$

where

$$\mathcal{H}_G \equiv -\frac{M_P^2}{2}\sqrt{\gamma}R^{(3)} - \frac{2}{M_P^2\sqrt{\gamma}}\left(\frac{1}{2}\Pi^2 - \Pi^{ij}\Pi_{ij}\right), \qquad \mathcal{H}_G^i \equiv -2(\partial_j\Pi^{ij} + \Gamma^i_{jk}\Pi^{jk}), \tag{4.8}$$

and

$$\mathcal{H}_M \equiv -\frac{G^{ab}}{4\lambda\sqrt{\gamma}}\Pi_a\Pi_b - \lambda\sqrt{\gamma}(\gamma^{ij}G_{ab}\partial_i\phi^a\partial_j\phi^b + 1) + \sqrt{\gamma}V(\phi^a), \qquad \mathcal{H}_M^i \equiv \Pi_a\partial^i\phi^a, \tag{4.9}$$

with $\Pi \equiv \Pi^i_i$.

Now, we have five primary constraints $(\Pi_{\mathcal{N}}, \Pi_i, \Pi_\lambda) \approx 0$[6] that are associated with nondynamical variables $(\mathcal{N}, \beta^i, \lambda)$, respectively. By taking into account these primary constraints and the action (4.7), we can construct the total Hamiltonian function from the standard definition in [75] as follows:

$$H_T = \int d^3x[\mathcal{N}(\mathcal{H}_G + \mathcal{H}_M) + \beta^i(\mathcal{H}_{Gi} + \mathcal{H}_{Mi}) + v_{\mathcal{N}}\Pi_{\mathcal{N}} + v^i\Pi_i + v_\lambda\Pi_\lambda], \tag{4.10}$$

where $v_{\mathcal{N}}$,v^i and v_λ are Lagrange multipliers which enforce the primary constraints. To identify the secondary constraints, we should check the time evolution of the primary constraints using the Poisson brackets [76]. For gravity and matter parts, the Poisson bracket is defined as

$$\begin{aligned}\{\mathcal{X},\mathcal{Y}\} \equiv \int d^3x\Bigg[&\frac{\delta\mathcal{X}}{\delta\mathcal{N}(x)}\frac{\delta\mathcal{Y}}{\delta\Pi_{\mathcal{N}}(x)} - \frac{\delta\mathcal{Y}}{\delta\mathcal{N}(x)}\frac{\delta\mathcal{X}}{\delta\Pi_{\mathcal{N}}(x)} + \frac{\delta\mathcal{X}}{\delta\beta^i(x)}\frac{\delta\mathcal{Y}}{\delta\Pi_i(x)} - \frac{\delta\mathcal{Y}}{\delta\beta^i(x)}\frac{\delta\mathcal{X}}{\delta\Pi_i(x)}\\ &+ \frac{\delta\mathcal{X}}{\delta\lambda(x)}\frac{\delta\mathcal{Y}}{\delta\Pi_\lambda(x)} - \frac{\delta\mathcal{Y}}{\delta\lambda(x)}\frac{\delta\mathcal{X}}{\delta\Pi_\lambda(x)} + \frac{\delta\mathcal{X}}{\delta\gamma_{ij}(x)}\frac{\delta\mathcal{Y}}{\delta\Pi^{ij}(x)} - \frac{\delta\mathcal{Y}}{\delta\gamma_{ij}(x)}\frac{\delta\mathcal{X}}{\delta\Pi^{ij}(x)} + \frac{\delta\mathcal{X}}{\delta\phi^a(x)}\frac{\delta\mathcal{Y}}{\delta\Pi_a(x)} - \frac{\delta\mathcal{Y}}{\delta\phi^a(x)}\frac{\delta\mathcal{X}}{\delta\Pi_a(x)}\Bigg].\end{aligned} \tag{4.11}$$

Thus one can easily examine the following fundamental Poisson brackets that hold between the canonical coordinates and momenta:

$$\begin{aligned}\{\lambda(\mathbf{x}), \Pi_\lambda(\mathbf{y})\} &= \delta^{(3)}(\mathbf{x}-\mathbf{y}),\\ \{\phi^a(\mathbf{x}), \Pi_b(\mathbf{y})\} &= \delta^a_b\delta^{(3)}(\mathbf{x}-\mathbf{y}),\\ \{\gamma_{ij}(\mathbf{x}), \Pi^{kl}(\mathbf{y})\} &= \frac{1}{2}(\delta^k_i\delta^l_j + \delta^l_i\delta^k_j)\delta^{(3)}(\mathbf{x}-\mathbf{y}).\end{aligned} \tag{4.12}$$

Let us now consider the time evolution of the primary constraint $\Upsilon_1 \equiv \Pi_\lambda \approx 0$ and check its consistency relations. We have

$$\Upsilon_2 \equiv \partial_t\Upsilon_1 = \{\Upsilon_1, H_T\} = -\frac{G^{ab}}{4\lambda^2\sqrt{\gamma}}\Pi_a\Pi_b + \sqrt{\gamma}(\gamma^{ij}G_{ab}\partial_i\phi^a\partial_i\phi^b + 1) \approx 0, \tag{4.13}$$

which is exactly the mimetic constraint (2.12) written in the ADM decomposition.

[6]Following [75], the notation ≈ 0 stands for the constraint equations.

From the above condition one immediately solves for the function λ,

$$\lambda = \left(\frac{G^{ab}}{4\sqrt{\gamma}}\Pi_a\Pi_b\right)^{1/2}[\sqrt{\gamma}(\gamma^{ij}G_{ab}\partial_i\phi^a\partial_j\phi^b + 1)]^{-1/2}. \tag{4.14}$$

The subsequent consistency relation gives

$$\begin{aligned}\Upsilon_3 &\equiv \partial_t\Upsilon_2 = \{\Upsilon_2, H_T\}\\ &= \Upsilon_3(\gamma_{ij}, \mathcal{N}, \beta^i, \lambda, \Pi_{ij}, \Pi_{\mathcal{N}}, \Pi_i, v_\lambda) \approx 0,\end{aligned} \tag{4.15}$$

which determines the Lagrangian multiplier v_λ in the terms of phase space variables and then the chain of constraints for primary constraint Υ_1 terminates here. This means that the set of 2 constraints Υ_1 and Υ_2 are second class. Now, by eliminating λ and Π_λ from the constraints $\Upsilon_1 \approx 0$ and $\Upsilon_2 \approx 0$, the dimension of the phase space reduce and so the reduced total Hamiltonian becomes

$$\begin{aligned}H_T^R = \int d^3x[&\mathcal{N}(\mathcal{H}_G + \mathcal{H}_M^R) + \beta^i(\mathcal{H}_{Gi} + \mathcal{H}_{Mi})\\ &+ v_{\mathcal{N}}\Pi_{\mathcal{N}} + v^i\Pi_i],\end{aligned} \tag{4.16}$$

where

$$\mathcal{H}_M^R \equiv \sqrt{\Pi_a\Pi^a}(\gamma^{ij}\partial_i\phi^a\partial_j\phi_a + 1)^{\frac{1}{2}} + \sqrt{\gamma}V(\phi^a). \tag{4.17}$$

Now we need to determine the Dirac bracket between the remaining phase space variables (γ_{ij}, $\mathcal{N}$, β^i, Π_{ij}, $\Pi_{\mathcal{N}}$, Π_i). The Dirac bracket between two phase space functions is defined as

$$\{\mathcal{X},\mathcal{Y}\}_D \equiv \{\mathcal{X},\mathcal{Y}\} - \sum_{I,J}\{\mathcal{X},\Phi_I\}(\mathcal{D}^{-1})^{IJ}\{\Phi_J,\mathcal{Y}\} \tag{4.18}$$

in which Φ^I, $I = 1, 2$ stand for the second class constraints $\Upsilon_1 \approx 0$, $\Upsilon_2 \approx 0$, and $\mathcal{D}_{IJ}$ is the matrix of the Poisson bracket between these constraints, i.e.,

$$\begin{aligned}\mathcal{D}_{11} &= \{\Upsilon_1(\mathbf{x}), \Upsilon_1(\mathbf{y})\} = 0,\\ \mathcal{D}_{12} &= -\mathcal{D}_{21} = \{\Upsilon_1(\mathbf{x}), \Upsilon_2(\mathbf{y})\} = \frac{\Pi_a(\mathbf{x})\Pi^a(\mathbf{x})}{\sqrt{\gamma}\lambda^3(\mathbf{x})}\delta^{(3)}(\mathbf{x}-\mathbf{y}),\\ \mathcal{D}_{22} &= \{\Upsilon_2(\mathbf{x}), \Upsilon_2(\mathbf{y})\}\\ &= \frac{1}{\lambda^2(\mathbf{x})}\Pi_b(\mathbf{x})\gamma^{ij}(\mathbf{y})\partial_{y^i}\phi^b(\mathbf{y})\partial_{y^j}\delta^{(3)}(\mathbf{x}-\mathbf{y}),\\ &\quad - \frac{1}{\lambda^2(\mathbf{y})}\Pi_b(\mathbf{y})\gamma^{ij}(\mathbf{x})\partial_{x^i}\phi^b(\mathbf{x})\partial_{x^j}\delta^{(3)}(\mathbf{x}-\mathbf{y}).\end{aligned} \tag{4.19}$$

Therefore, the matrix $\mathcal{D}$ and its inverse $\mathcal{D}^{-1}$ can be written schematically as [77]

$$\mathcal{D} = \begin{pmatrix} 0 & A\\ -A & B\end{pmatrix}, \qquad \mathcal{D}^{-1} = \begin{pmatrix} A^{-1}BA^{-1} & -A^{-1}\\ A^{-1} & 0\end{pmatrix}. \tag{4.20}$$

Keeping the above forms in mind and considering the fact that $\{\gamma_{ij}, \Pi_\lambda\} = \{\Pi^{ij}, \Pi_\lambda\} = \{\Pi_a, \Pi_\lambda\} = \{\phi^a, \Pi_\lambda\} = 0$, one finds that the Dirac brackets coincides with the Poisson brackets.

Now we proceed to the analysis of the consistency relation for the primary constraints $\Omega_1 \equiv \Pi_{\mathcal{N}} \approx 0$ and $\Gamma_1^i \equiv \Pi^i \approx 0$. The time evolution of these constraints gives the secondary constraints

$$\begin{aligned}\Omega_2 &\equiv \partial_t\Omega_1 = \{\Omega_1(\mathbf{x}), H_T^R(\mathbf{y})\}\\ &= -(\mathcal{H}_G + \mathcal{H}_M^R)\delta^3(\mathbf{x}-\mathbf{y}) \approx 0,\\ \Gamma_2^i &\equiv \partial_t\Gamma_1^i = \{\Gamma_1^i(\mathbf{x}), H_T^R(\mathbf{y})\}\\ &= -(\mathcal{H}_G{}^i(\mathbf{x}) + \mathcal{H}_M{}^i(\mathbf{x}))\delta^3(\mathbf{x}-\mathbf{y}) \approx 0.\end{aligned} \tag{4.21}$$

Requiring these constraints to be time independent yields

$$\begin{aligned}\Omega_3 &= \partial_t\Omega_2 = \{\Omega_2(\mathbf{x}), H_T^R(\mathbf{y})\}\\ &= -\mathcal{N}\{\Omega_2(\mathbf{x}),\Omega_2(\mathbf{y})\} - \beta_i\{\Omega_2(\mathbf{x}),\Gamma_2^i(\mathbf{y})\} \approx 0,\\ \Gamma_3^i &= \partial_t\Gamma_2^i = \{\Gamma_2^i(\mathbf{x}), H_T^R(\mathbf{y})\}\\ &= -\mathcal{N}\{\Gamma_2^i(\mathbf{x}),\Omega_2(\mathbf{y})\} - \beta_j\{\Gamma_2^i(\mathbf{x}),\Gamma_2^j(\mathbf{y})\} \approx 0,\end{aligned} \tag{4.22}$$

where

$$\begin{aligned}\{\Omega_2(\mathbf{x}), \Omega_2(\mathbf{y})\} &= \Gamma_2^i(\mathbf{y})\partial_{x^i}\delta^{(3)}(\mathbf{x}-\mathbf{y})\\ &\quad - \Gamma_2^j(\mathbf{x})\partial_{y^j}\delta^{(3)}(\mathbf{x}-\mathbf{y}) \approx 0,\\ \{\Omega_2(\mathbf{x}), \Gamma_2^i(\mathbf{y})\} &= -\Omega_2\partial_{x_i}\delta^{(3)}(\mathbf{x}-\mathbf{y}) \approx 0,\\ \{\Gamma_2^i(\mathbf{x}), \Gamma_2^j(\mathbf{y})\} &= \Gamma_2^i(\mathbf{y})\partial_{x_j}\delta^{(3)}(\mathbf{x}-\mathbf{y})\\ &\quad - \Gamma_2^j(\mathbf{x})\partial_{y_i}\delta^{(3)}(\mathbf{x}-\mathbf{y}) \approx 0.\end{aligned} \tag{4.23}$$

Clearly, the above Poisson algebras vanish on the constraint surface (see Appendix A for more details). Indeed, the time evolution of the secondary constraints Ω_2 and Γ_2^i determine none of the Lagrangian multipliers and do not generate any additional constraints. Consequently these eight constraints Ω_1, Ω_2, Γ_1^i, and Γ_2^i are all first class constraints, which are interpreted as the generators of diffeomorphism.

Now the DOFs in phase space can be read off from the master formula of the constrained system as [76]

$$\text{DOF} = N - 2\#\text{1st Class} - \#\text{2nd Class}, \tag{4.24}$$

in which N is the total number of phase space variables. In our model, we have 20 phase space variables containing $(\mathcal{N}, \beta^i, \gamma_{ij}, \Pi_{\mathcal{N}}, \Pi^i, \Pi_{ij})$, two variables for (λ, Π_λ), and $\mathcal{M}$ total number of the conjugate pair (ϕ^a, Π_a). Correspondingly, the number of DOFs is obtained to be

$$\mathrm{DOF} = (20 + 2 + \mathcal{M}) - 16 - 2 = 4 + \mathcal{M}, \quad (4.25)$$

which corresponds to $(4+\mathcal{M})/2$ physical degrees of freedom in the configuration space.

Note that $\mathcal{M}/2$ represents the dimension of the field space manifold or equivalently the number of scalar fields. Thus, in addition to the two gravitational degrees of freedom of general relativity, there exists $\mathcal{M}/2$ extra physical degree of freedom. This finding implies that the theory is free from the so-called Ostrogradsky ghost [78]. In fact, the Ostrogradsky ghost arises when the higher derivative terms increase the number of degrees of freedom for the system under consideration.

As an example, for two-field mimetic case spanning a 2D curved field space ($\mathcal{M}=2$), we have 4 DOFs corresponding to one adiabatic mode, one entropy mode and two tensor modes as verified perturbatively in previous section.

V. CONCLUSIONS

In this paper we have extended the idea of mimetic gravity to multifield setup with the curved field space manifold. Motivated from the single field case, we have constructed the multifield mimetic setup via the conformal transformation between the physical and the original auxiliary metrics. Solving the eigentensor equation for the Jacobian of such a transformation, we have found the associated eigentensors and eigenvalues. The multifield generalization of the mimetic scenario can be interpreted as the singular limit of the conformal transformation by demanding that the kinetic type eigenvalues to be zero.

At the cosmological background, as expected, the energy density of the multifield mimetic scenario indeed plays the role of dark mater similar to the original single field setup. At the perturbation level, we have employed the kinematic basis in which the perturbations are decomposed into the tangential and the perpendicular to the field space trajectory. By considering the perturbations in the kinematic basis, we performed explicit perturbation analysis in the spatially flat gauge for two-field mimetic case. We have found that the perturbation mode perpendicular to background trajectory in the field space manifold, u_N, is excited, whereas the perturbation mode tangential to the background trajectory, u_T, does not propagate. More precisely, the entropy mode, originated from the extra scalar field in our model, propagates with the sound speed equal to unity, whereas the sound speed for the adiabatic mode is zero. This is consistent with the fact that the mimetic background describes a dark-matter fluid. In addition, whether or not the entropy perturbation is healthy directly depends on the signature of the field-space metric G_{ab}. In the case of the field space with an Euclidean signature, the entropy mode is healthy, whereas in the case of the Lorentzian manifold, the entropy perturbation suffers from the ghost and gradient instabilities.

Although one of the modes does not propagate at the linear perturbation level but it contributes to the physical DOFs of the model. We further confirmed this result by performing the full nonlinear Hamiltonian analysis of the multifield mimetic theory and verified the correct number of DOFs necessary to prevent the presence of the Ostrogradsky-type ghost.

ACKNOWLEDGMENTS

We would like to thank Mohammad Ali Gorji for insightful discussions. H. F. and A. T. acknowledge the partial support from the "Saramadan" federation of Iran.

APPENDIX A: CONSTRAINT ALGEBRA

Using the Poisson bracket relations (4.11), here we check the constraint $\Omega_2 \equiv -\mathcal{H}_G - \mathcal{H}_M^R$ and $\Gamma_2^i \equiv -\mathcal{H}_G^i - \mathcal{H}_M^i$ in a closed algebra [75,76]. The gravity part $\mathcal{H}_G^i$ are the generators of three-dimensional diffeomorphism and the other gravity part $\mathcal{H}_G$ is a scalar with respect to spatial diffeomorphism [58], then $\mathcal{H}_G$ and $\mathcal{H}_G^i$ satisfy

$$\begin{aligned}
\{\mathcal{H}_G(\mathbf{x}), \mathcal{H}_G(\mathbf{y})\} &= \mathcal{H}_G^i(\mathbf{y})\partial_{x^i}\delta^{(3)}(\mathbf{x}-\mathbf{y}) \\
&\quad - \mathcal{H}_G^j(\mathbf{x})\partial_{y^j}\delta^{(3)}(\mathbf{x}-\mathbf{y}), \\
\{\mathcal{H}_G(\mathbf{x}), \mathcal{H}_G^i(\mathbf{y})\} &= -\mathcal{H}_G\partial_i\delta^{(3)}(\mathbf{x}-\mathbf{y}), \\
\{\mathcal{H}_G^i(\mathbf{x}), \mathcal{H}_G^j(\mathbf{y})\} &= \mathcal{H}_G^i(\mathbf{y})\partial_{x_j}\delta^{(3)}(\mathbf{x}-\mathbf{y}) \\
&\quad - \mathcal{H}_G^j(\mathbf{x})\partial_{y_i}\delta^{(3)}(\mathbf{x}-\mathbf{y}). \qquad (A1)
\end{aligned}$$

For the matter part, i.e., $\mathcal{H}_M^R$ and $\mathcal{H}_M^i$, similarly one obtains

$$\begin{aligned}
\{\mathcal{H}_M^R(\mathbf{x}), \mathcal{H}_M^R(\mathbf{y})\} &= \mathcal{H}_M^i(\mathbf{y})\partial_{x^i}\delta^{(3)}(\mathbf{x}-\mathbf{y}) \\
&\quad - \mathcal{H}_M^j(\mathbf{x})\partial_{y^j}\delta^{(3)}(\mathbf{x}-\mathbf{y}), \\
\{\mathcal{H}_M^R(\mathbf{x}), \mathcal{H}_M^i(\mathbf{y})\} &= -\mathcal{H}_M^R\partial_{x_i}\delta^{(3)}(\mathbf{x}-\mathbf{y}), \\
\{\mathcal{H}_M^i(\mathbf{x}), \mathcal{H}_M^j(\mathbf{y})\} &= \mathcal{H}_M^i(\mathbf{y})\partial_{x_j}\delta^{(3)}(\mathbf{x}-\mathbf{y}) \\
&\quad - \mathcal{H}_M^j(\mathbf{x})\partial_{y_i}\delta^{(3)}(\mathbf{x}-\mathbf{y}). \qquad (A2)
\end{aligned}$$

Therefore, the total constraints $\Omega_2 \equiv -\mathcal{H}_G - \mathcal{H}_M^R$ and $\Gamma_2^i \equiv -\mathcal{H}_G^i - \mathcal{H}_M^i$ also form the closed algebra,

$$\begin{aligned}
\{\Omega_2(\mathbf{x}), \Omega_2(\mathbf{y})\} &= \Gamma_2^i(\mathbf{y})\partial_{x^i}\delta^{(3)}(\mathbf{x}-\mathbf{y}) \\
&\quad - \Gamma_2^j(\mathbf{x})\partial_{y^j}\delta^{(3)}(\mathbf{x}-\mathbf{y}), \\
\{\Omega_2(\mathbf{x}), \Gamma_2^i(\mathbf{y})\} &= -\Omega_2\partial_{x_i}\delta^{(3)}(\mathbf{x}-\mathbf{y}), \\
\{\Gamma_2^i(\mathbf{x}), \Gamma_2^j(\mathbf{y})\} &= \Gamma_2^i(\mathbf{y})\partial_{x_j}\delta^{(3)}(\mathbf{x}-\mathbf{y}) \\
&\quad - \Gamma_2^j(\mathbf{x})\partial_{y_i}\delta^{(3)}(\mathbf{x}-\mathbf{y}). \qquad (A3)
\end{aligned}$$

APPENDIX B: QUADRATIC ACTION IN THE COMOVING GAUGE

In comoving gauge ψ is turned on in the scalar perturbations (3.3). In this respect, the equation of motion for the nondynamical mode B leads to the following constraint,

$$\alpha = \frac{\dot{\psi}}{H} + \epsilon H Q_a \dot{\phi}_0^a. \tag{B1}$$

By imposing the above relation in the corresponding quadratic action, one obtains

$$\begin{aligned} S^2 = \int d^3x dt a^3 \Big[& M_P^2 \epsilon H^2 G_{bc} D_t Q^b D_t Q^c - 2M_P^2 \epsilon^2 H^3 Q_b D_t Q_c \dot{\phi}_0^b \dot{\phi}_0^c - M_{bc}^2 Q^b Q^c \\ & - \frac{M_P^2}{a^2} \epsilon H^2 G_{bc} \partial_i Q^b \partial^i Q^c + 2\delta\lambda \left(\epsilon H Q_b \dot{\phi}_0^b - D_t Q_b \dot{\phi}_0^b + \frac{\dot{\psi}}{H} \right) + M_P^2 \epsilon \dot{\psi}^2 \\ & - \psi (3Q^b V_b - 6M_P^2 \epsilon H^2 D_t Q_b \dot{\phi}_0^b) - \frac{M_P^2}{a^2} \epsilon \partial^2 \psi \left(\psi + 2HQ_b \dot{\phi}_0^b + 2\frac{\dot{\psi}}{H} \right) \\ & - \dot{\psi} \left(\frac{V_d Q^d}{H} - 2M_P^2 \epsilon^2 H^2 Q_b \dot{\phi}_0^b + 2M_P^2 \epsilon H D_t Q_b \dot{\phi}_0^b \right) \Big], \end{aligned} \tag{B2}$$

where the mass matrix M_{ab} was defined in Eq. (3.21). Now, we can decompose the variable Q^a into the directions along and orthogonal to time evolution [79] as

$$Q^a = Q_\perp^a + \dot{\phi}_0^a \tilde{\pi}, \tag{B3}$$

with the orthogonality condition $G_{ab} \dot{\phi}_0^a Q_\perp^a = 0$. In the comoving gauge we impose $\tilde{\pi} = 0$. It should be noted that the $\tilde{\pi}$ mode is the fluctuation in the direction of the time translation, and is interpreted as the Goldstone mode appearing from the spontaneous breaking of time translation invariant [80]. Moreover, the orthogonal modes, $Q_\perp^a$, are gauge invariant quantities and are usually called "isocurvature" modes [72]. Similar to the single field inflation, one can introduce the Mukhanov-Sasaki variable as [57]

$$\tilde{Q}^a \equiv Q^a - \frac{\dot{\phi}_0^a}{H} \psi = Q_\perp^a - \frac{\dot{\phi}_0^a}{H} (\psi - H\tilde{\pi}) \equiv Q_\perp^a - \frac{\dot{\phi}_0^a}{H} \pi \tag{B4}$$

or equivalently

$$Q^a \equiv Q_\perp^a - \frac{\dot{\phi}_0^a}{H} (\pi - \psi). \tag{B5}$$

In two-field case, due to the orthogonality condition, the mode $Q_\perp^a$ is proportional to the normal vector N^a, i.e., $Q_\perp^a \propto N^a$, and one takes the amplitude of $Q_\perp$ as the isocurvature field $\mathcal{F}$ [57]. Moreover, in comoving gauge ($\tilde{\pi} = 0$) in which $\psi = R$, one can replace π simply with the curvature perturbation $\mathcal{R}$.

In this regard, the variation of the quadratic action (B2) with respect to $\delta\lambda$, in comoving gauge, yields the constraint

$$\dot{\mathcal{R}} = -H \dot{\theta} \mathcal{F}. \tag{B6}$$

By imposing the above constraint and Eq. (B5) into the quadratic action (B2), finally we arrive at the quadratic action in comoving gauge,

$$\begin{aligned} S^2 = \int \mathrm{d}x^3\, \mathrm{d}t a^3 M_P^2 \epsilon H^2 \Big[& \mathrm{sgn}(\pm 1) \left(\dot{\mathcal{F}}^2 - \frac{1}{a^2} (\partial \mathcal{F})^2 \right) \\ & - \left(\frac{M_{NN}^2}{M_P^2 \epsilon H^2} + 2\dot{\theta}^2 \right) \mathcal{F}^2 \\ & + \frac{2\dot{\theta}}{a^2 \epsilon H^2} \mathcal{F} \partial^2 \mathcal{R} + \frac{1}{\epsilon H^2 a^2} (\partial \mathcal{R})^2 \Big]. \end{aligned} \tag{B7}$$

It implies that the curvature perturbation $\mathcal{R}$ does not propagate in our setup. Clearly, the stability of perturbations depends on the signature of the metric G_{ab}. In the case of the field space with an Euclidean signature [$\mathrm{sgn}(+1) = 1$], the isocurvature mode does not suffer from ghost and gradient instabilities, whereas in the case of the Lorentzian manifold with $\mathrm{sgn}(-1) = -1$, the isocurvature perturbation is pathological. In 2D flat field space, our results are in agreement with those in [23].

[1] A. H. Chamseddine and V. Mukhanov, Mimetic dark matter, J. High Energy Phys. 11 (2013) 135.
[2] A. H. Chamseddine, V. Mukhanov, and A. Vikman, Cosmology with mimetic matter, J. Cosmol. Astropart. Phys. 06 (2014) 017.
[3] A. H. Chamseddine and V. Mukhanov, Resolving cosmological singularities, J. Cosmol. Astropart. Phys. 03 (2017) 009.
[4] A. H. Chamseddine and V. Mukhanov, Nonsingular black hole, Eur. Phys. J. C **77**, 183 (2017).
[5] N. Deruelle and J. Rua, Disformal transformations, veiled general relativity and mimetic gravity, J. Cosmol. Astropart. Phys. 09 (2014) 002.
[6] F.-F. Yuan and P. Huang, Induced geometry from disformal transformation, Phys. Lett. B **744**, 120 (2015).
[7] H. Firouzjahi, M. A. Gorji, S. A. Hosseini Mansoori, A. Karami, and T. Rostami, Two-field disformal transformation and mimetic cosmology, J. Cosmol. Astropart. Phys. 11 (2018) 046.
[8] L. Mirzagholi and A. Vikman, Imperfect dark matter, J. Cosmol. Astropart. Phys. 06 (**2015**) 028.
[9] R. Myrzakulov, L. Sebastiani, S. Vagnozzi, and S. Zerbini, Static spherically symmetric solutions in mimetic gravity: Rotation curves and wormholes, Classical Quantum Gravity **33**, 125005 (2016).
[10] F. Arroja, N. Bartolo, P. Karmakar, and S. Matarrese, Cosmological perturbations in mimetic Horndeski gravity, J. Cosmol. Astropart. Phys. 04 (2016) 042.
[11] L. Sebastiani, S. Vagnozzi, and R. Myrzakulov, Mimetic gravity: A review of recent developments and applications to cosmology and astrophysics, Adv. High Energy Phys. **2017**, 3156915 (2017).
[12] J. Dutta, W. Khyllep, E. N. Saridakis, N. Tamanini, and S. Vagnozzi, Cosmological dynamics of mimetic gravity, J. Cosmol. Astropart. Phys. 02 (**2018**) 041.
[13] H. Saadi, A cosmological solution to mimetic dark matter, Eur. Phys. J. C **76**, 14 (2016).
[14] M. A. Gorji, A. Allahyari, M. Khodadi, and H. Firouzjahi, Mimetic black holes, Phys. Rev. D **101**, 124060 (2020).
[15] J. Matsumoto, S. D. Odintsov, and S. V. Sushkov, Cosmological perturbations in a mimetic matter model, Phys. Rev. D **91**, 064062 (2015).
[16] D. Momeni, K. Myrzakulov, R. Myrzakulov, and M. Raza, Cylindrical solutions in mimetic gravity, Eur. Phys. J. C **76**, 301 (2016).
[17] A. V. Astashenok and S. D. Odintsov, From neutron stars to quark stars in mimetic gravity, Phys. Rev. D **94**, 063008 (2016).
[18] N. Sadeghnezhad and K. Nozari, Braneworld mimetic cosmology, Phys. Lett. B **769**, 134 (2017).
[19] M. A. Gorji, S. Mukohyama, H. Firouzjahi, and S. A. Hosseini Mansoori, Gauge field mimetic cosmology, J. Cosmol. Astropart. Phys. 08 (**2018**) 047.
[20] M. A. Gorji, S. Mukohyama, and H. Firouzjahi, Cosmology in mimetic SU(2) gauge theory, J. Cosmol. Astropart. Phys. 05 (2019) 019.
[21] K. Nozari and N. Rashidi, Mimetic DBI inflation in confrontation with Planck2018 data, Astrophys. J. **882**, 78 (2019).
[22] A. R. Solomon, V. Vardanyan, and Y. Akrami, Massive mimetic cosmology, Phys. Lett. B **794**, 135 (2019).
[23] L. Shen, Y. Zheng, and M. Li, Two-field mimetic gravity revisited and Hamiltonian analysis, J. Cosmol. Astropart. Phys. 12 (2019) 026.
[24] A. Ganz, N. Bartolo, and S. Matarrese, Towards a viable effective field theory of mimetic gravity, J. Cosmol. Astropart. Phys. 12 (2019) 037.
[25] M. de Cesare, Reconstruction of mimetic gravity in a non-singular bouncing universe from quantum gravity, Universe **5**, 107 (2019).
[26] K. Nozari and N. Sadeghnezhad, Braneworld mimetic $f(R)$ gravity, Int. J. Geom. Methods Mod. Phys. **16**, 1950042 (2019).
[27] M. de Cesare, Limiting curvature mimetic gravity for group field theory condensates, Phys. Rev. D **99**, 063505 (2019).
[28] A. Ganz, P. Karmakar, S. Matarrese, and D. Sorokin, Hamiltonian analysis of mimetic scalar gravity revisited, Phys. Rev. D **99**, 064009 (2019).
[29] A. Ganz, N. Bartolo, P. Karmakar, and S. Matarrese, Gravity in mimetic scalar-tensor theories after GW170817, J. Cosmol. Astropart. Phys. 01 (**2019**) 056.
[30] A. Sheykhi and S. Grunau, Topological black holes in mimetic gravity, Int. J. Mod. Phys. A **36**, 2150186 (2021).
[31] A. Sheykhi, Mimetic gravity in $(2+1)$-dimensions, J. High Energy Phys. 01 (2021) 043.
[32] A. Sheykhi, Mimetic black strings, J. High Energy Phys. 07 (2020) 031.
[33] A. V. Astashenok, S. D. Odintsov, and V. K. Oikonomou, Modified Gauss–Bonnet gravity with the Lagrange multiplier constraint as mimetic theory, Classical Quantum Gravity **32**, 185007 (2015).
[34] S. Nojiri, S. D. Odintsov, and V. K. Oikonomou, Unimodular-mimetic cosmology, Classical Quantum Gravity **33**, 125017 (2016).
[35] S. Nojiri, S. D. Odintsov, and V. K. Oikonomou, Ghost-free $F(R)$ gravity with Lagrange multiplier constraint, Phys. Lett. B **775**, 44 (2017).
[36] S. Nojiri, S. D. Odintsov, and V. K. Oikonomou, Viable mimetic completion of unified inflation-dark energy evolution in modified gravity, Phys. Rev. D **94**, 104050 (2016).
[37] S. D. Odintsov and V. K. Oikonomou, The reconstruction of $f(\phi)R$ and mimetic gravity from viable slow-roll inflation, Nucl. Phys. **B929**, 79 (2018).
[38] A. Casalino, M. Rinaldi, L. Sebastiani, and S. Vagnozzi, Alive and well: Mimetic gravity and a higher-order extension in light of GW170817, Classical Quantum Gravity **36**, 017001 (2019).
[39] S. Bhattacharjee, Inflation in mimetic $f(R,T)$ gravity, New Astron. **90**, 101657 (2022).
[40] F. Izaurieta, P. Medina, N. Merino, P. Salgado, and O. Valdivia, Mimetic Einstein-Cartan-Sciama-Kibble (ECSK) gravity, J. High Energy Phys. 10 (2020) 150.
[41] M. de Cesare, S. S. Seahra, and E. Wilson-Ewing, The singularity in mimetic Kantowski-Sachs cosmology, J. Cosmol. Astropart. Phys. 07 (**2020**) 018.
[42] A. Z. Kaczmarek and D. Szczęśniak, Cosmology in the mimetic higher-curvature $f(R, R_{\mu\nu}R^{\mu\nu})$ gravity, Sci. Rep. **11**, 18363 (2021).

[43] A. Barvinsky, Dark matter as a ghost free conformal extension of Einstein theory, J. Cosmol. Astropart. Phys. 01 (2014) 014.

[44] M. Chaichian, J. Kluson, M. Oksanen, and A. Tureanu, Mimetic dark matter, ghost instability and a mimetic tensor-vector-scalar gravity, J. High Energy Phys. 12 (2014) 102.

[45] F. Capela and S. Ramazanov, Modified dust and the small scale crisis in CDM, J. Cosmol. Astropart. Phys. 04 (2015) 051.

[46] A. De Felice and S. Mukohyama, Phenomenology in minimal theory of massive gravity, J. Cosmol. Astropart. Phys. 04 (2016) 028.

[47] A. E. Gümrükccüoğlu, S. Mukohyama, and T. P. Sotiriou, Low energy ghosts and the Jeans' instability, Phys. Rev. D **94**, 064001 (2016).

[48] E. Babichev and S. Ramazanov, Gravitational focusing of imperfect dark matter, Phys. Rev. D **95**, 024025 (2017).

[49] E. Babichev and S. Ramazanov, Caustic free completion of pressureless perfect fluid and k-essence, J. High Energy Phys. 08 (2017) 040.

[50] A. Ijjas, J. Ripley, and P. J. Steinhardt, NEC violation in mimetic cosmology revisited, Phys. Lett. B **760**, 132 (2016).

[51] H. Firouzjahi, M. A. Gorji, and S. A. Hosseini Mansoori, Instabilities in mimetic matter perturbations, J. Cosmol. Astropart. Phys. 07 (2017) 031.

[52] Y. Zheng, L. Shen, Y. Mou, and M. Li, On (in)stabilities of perturbations in mimetic models with higher derivatives, J. Cosmol. Astropart. Phys. 08 (**2017**) 040.

[53] S. Hirano, S. Nishi, and T. Kobayashi, Healthy imperfect dark matter from effective theory of mimetic cosmological perturbations, J. Cosmol. Astropart. Phys. 07 (2017) 009.

[54] M. A. Gorji, S. A. Hosseini Mansoori, and H. Firouzjahi, Higher derivative mimetic gravity, J. Cosmol. Astropart. Phys. 01 (2018) 020.

[55] S. A. Hosseini Mansoori, A. Talebian, and H. Firouzjahi, Mimetic inflation, J. High Energy Phys. 01 (2021) 183.

[56] J.-O. Gong and T. Tanaka, A covariant approach to general field space metric in multi-field inflation, J. Cosmol. Astropart. Phys. 03 (2011) 015.

[57] J.-O. Gong, Multi-field inflation and cosmological perturbations, Int. J. Mod. Phys. D **26**, 1740003 (2017).

[58] J.-O. Gong, M.-S. Seo, and G. Shiu, Path integral for multi-field inflation, J. High Energy Phys. 07 (2016) 099.

[59] S. Cespedes, V. Atal, and G. A. Palma, On the importance of heavy fields during inflation, J. Cosmol. Astropart. Phys. 05 (2012) 008.

[60] A. Achúcarro, V. Atal, C. Germani, and G. A. Palma, Cumulative effects in inflation with ultra-light entropy modes, J. Cosmol. Astropart. Phys. 02 (2017) 013.

[61] S. Mizuno and S. Mukohyama, Primordial perturbations from inflation with a hyperbolic field-space, Phys. Rev. D **96**, 103533 (2017).

[62] J. Fumagalli, S. Garcia-Saenz, L. Pinol, S. Renaux-Petel, and J. Ronayne, Hyper-Non-Gaussianities in Inflation with Strongly Nongeodesic Motion, Phys. Rev. Lett. **123**, 201302 (2019).

[63] S. Garcia-Saenz, L. Pinol, and S. Renaux-Petel, Revisiting non-Gaussianity in multifield inflation with curved field space, J. High Energy Phys. 01 (2020) 073.

[64] A. Achúcarro and Y. Welling, Orbital Inflation: Inflating along an angular isometry of field space, arXiv:1907.02020.

[65] Y. Akrami, M. Sasaki, A. R. Solomon, and V. Vardanyan, Multi-field dark energy: Cosmic acceleration on a steep potential, Phys. Lett. B **819**, 136427 (2021).

[66] R. Arnowitt, S. Deser, and C. W. Misner, Republication of: The dynamics of general relativity, Gen. Relativ. Gravit. **40**, 1997 (2008).

[67] M. Zumalacárregui and J. García-Bellido, Transforming gravity: From derivative couplings to matter to second-order scalar-tensor theories beyond the Horndeski Lagrangian, Phys. Rev. D **89**, 064046 (2014).

[68] M. A. Gorji, A. Allahyari, M. Khodadi, and H. Firouzjahi, Mimetic black holes, Phys. Rev. D **101**, 124060 (2020).

[69] A. Golovnev, On the recently proposed mimetic dark matter, Phys. Lett. B **728**, 39 (2014).

[70] J. Elliston, D. Seery, and R. Tavakol, The inflationary bispectrum with curved field-space, J. Cosmol. Astropart. Phys. 11 (2012) 060.

[71] E. McDonough, A. H. Guth, and D. I. Kaiser, Nonminimal couplings and the forgotten field of axion inflation, arXiv:2010.04179.

[72] C. Gordon, D. Wands, B. A. Bassett, and R. Maartens, Adiabatic and entropy perturbations from inflation, Phys. Rev. D **63**, 023506 (2000).

[73] G. W. Horndeski, Second-order scalar-tensor field equations in a four-dimensional space, Int. J. Theor. Phys. **10**, 363 (1974).

[74] J. Ben Achour, M. Crisostomi, K. Koyama, D. Langlois, K. Noui, and G. Tasinato, Degenerate higher order scalar-tensor theories beyond Horndeski up to cubic order, J. High Energy Phys. 12 (2016) 100.

[75] M. Bojowald, *Canonical Gravity and Applications: Cosmology, Black Holes, and Quantum Gravity* (Cambridge University Press, Cambridge, England, 2010).

[76] P. Dirac, *Lectures on Quantum Mechanics* (Belfer Graduate School of Science, Yeshiva University Press, New York, 1964).

[77] M. Chaichian, J. Klusoň, M. Oksanen, and A. Tureanu, Mimetic dark matter, ghost instability and a mimetic tensor-vector-scalar gravity, J. High Energy Phys. 12 (2014) 102.

[78] R. P. Woodard, Ostrogradsky's theorem on Hamiltonian instability, Scholarpedia **10**, 32243 (2015).

[79] A. Achucarro, J.-O. Gong, S. Hardeman, G. A. Palma, and S. P. Patil, Effective theories of single field inflation when heavy fields matter, J. High Energy Phys. 05 (2012) 066.

[80] C. Cheung, P. Creminelli, A. Fitzpatrick, J. Kaplan, and L. Senatore, The effective field theory of inflation, J. High Energy Phys. 03 (2008) 014.